ELSEVIER

Marine and Petroleum Geology 21 (2004) 41–62

Marine and Petroleum Geology

www.elsevier.com/locate/marpetgeo

Hydrocarbon potential of the Meso-Cenozoic Turkana Depression, northern Kenya. I. Reservoirs: depositional environments, diagenetic characteristics, and source rock–reservoir relationships

J.-J. Tiercelin[a,b,*], J.-L. Potdevin[c], C.K. Morley[d], M.R. Talbot[e], H. Bellon[a,b], A. Rio[a,b], B. Le Gall[a,b], W. Vétel[a,b]

[a]*UMR CNRSUBO 6538 Domaines Océaniques, Institut Universitaire Européen de la Mer, Place Nicolas Copernic, 29280 Plouzané, France*
[b]*Université de Bretagne Occidentale, 6, avenue Le Gorgeu, B.P. 809, 29285 Brest, France*
[c]*Université des Sciences et Technologies de Lille, UFR des Sciences de la Terre, UMR CNRS Processus et Bilans des Domaines Sédimentaires 59655 Villeneuve d'Ascq Cedex, France*
[d]*Universiti Brunei Darussalam, Jalan Tungku Link, Gadong, BE1410 Negara Brunei Darussalam*
[e]*Geological Institute, University of Bergen, Allégt. 41, 5007 Bergen, Norway*

Received 14 March 2003; received in revised form 12 November 2003; accepted 14 November 2003

Abstract

Major oil exploration efforts started in the 70s in the Meso-Cenozoic Anza Rift and Cenozoic Turkana Depression of northern Kenya. Thick piles of fluvio-lacustrine sandstones and shales infill these different rift basins. West of Lake Turkana, the Auwerwer/Lomerimong Formation is part of the Palaeogene–middle Miocene age, 7 km-thick fluvio-lacustrine infill of the Lokichar half-graben. East of Lake Turkana, the 220 m-thick Sera Iltomia Formation is of possible late Mesozoic–basal Palaeocene age, and comprises sandstones and mudstones with conglomeratic layers. The poorly dated Sera Iltomia Formation may represent either the early phase of Cenozoic East African rifting in northern Kenya or the Meso-Cenozoic Anza Rift.

The sandstones of these two formations exhibit different sediment sources and consequent reservoir quality. The Sera Iltomia sandstones are immature and basement-derived. While the sources of clastic material from the Auwerwer/Lomerimong section originated from both volcanic and basement terrains. Palaeocurrent data for the Sera Iltomia and Auwerwer/Lomerimong basement-derived sandstones suggest a source to the south and south-east of Lake Turkana. The volcanic-derived clastic rocks forming part of the Auwerwer/Lomerimong section suggest a sediment source to the south-southeast of the Lokichar Basin, linked to the lower Miocene Samburu Basalts Formation. Evidence for significant burial diagenesis is absent in both. In the Auwerwer/Lomerimong sandstones, calcite–analcite precipitation and calcite cementation significantly reduced the porosity from initial values of 40–45% to values which ranges up to 15%. In the Sera Iltomia sandstones, different early diagenetic events are recorded by calcite, quartz or kaolin cements. Quartz overgrowths and kaolin precipitation are local phenomena, and did not induce significant porosity reduction. In some cases, calcite cementation completely occluded the initial porosity, but in other cases it has helped preserve significant porosity by limiting mechanical compaction. This cementation resulted in a higher porosity (up to 33%) than in the Lomerimong sandstones and a better potential to form reservoirs of good quality. Comparison with potential reservoirs encountered in the Anza Rift wells demonstrate that volcaniclastic-rich sandstones are more frequently affected by pore cementation rather than the arkosic-type sandstones. The complex stratigraphic and structural organization of the Turkana Depression/Anza Rift system illustrates the potential variability in sediment source, diagenesis and reservoir–source rock relationships when exploring for reservoirs in continental rift systems.

Keywords: Turkana depression; Anza Rift; Meso-Cenozoic; Fluvio-lacustrine sandstone; Reservoir characteristic

1. Introduction

A large number of major oil provinces over the world are known to have been initiated from source rocks of lacustrine origin (Fleet, Kelts, & Talbot, 1988; Gibling, 1988; Katz,

* Corresponding author. Tel.: +33-2-98-49-87-59; fax: +33-2-98-49-87-49..
E-mail addresses: jjtierc@univ-brest.fr (J.-J. Tiercelin).

0264-8172/$ - see front matter © 2003 Published by Elsevier Ltd.
doi:10.1016/j.marpetgeo.2003.11.007

1990). Similarly, fluvial and fluvio-deltaic sandstone bodies are known as important hydrocarbon reservoirs, especially when they are linked with lacustrine basins (Qiu, Xue, & Xiao, 1987). Most of the corresponding lake basins are assumed to have developed within extensional continental settings such as those lying along the two branches of the Cenozoic East African Rift System (EARS) (Katz, 1995; Lambiase, 1995; Morley, 1995, 1999b; Tiercelin, 1991). Sediments showing good source rock quality have been observed in several of the modern large (Albert, Edward, Kivu, Tanganyika) and small (Bogoria) lakes of the EARS (Herbin, 1979; Huc, Le Fournier, Vandenbroucke, & Bessereau, 1990; Katz, 1988; Talbot, 1988; Tiercelin & Vincens, 1987). Petroleum occurrences have also been observed in some of these lake basins (Albert, Tanganyika, Bogoria) (Harris, Pallister, & Brown, 1956; Grall, 2000; Simoneit, Aboul-Kassim, & Tiercelin, 2000; Tiercelin et al., 1993) (Fig. 1).

Major exploration efforts have been carried out since the 70s by several oil companies in the Eastern and Western branches of the EARS, and particularly in the northern and central Kenya Rift (Bosworth, 1992; Bosworth & Maurin, 1993; Bosworth & Morley, 1994; Morley et al., 1992, 1999b; Mugisha, Ebinger, Strecker, & Pope, 1997) (Fig. 1). Extensive seismic investigation of the Turkana Depression by Project PROBE (offshore Lake Turkana) (Dunkelman, Karson, & Rosendahl, 1988, Dunkelman, Rosendahl, & Karson, 1989) and by Amoco Kenya Petroleum Company (Morley et al., 1992, 1999b) have revealed the existence of several N-S-trending half-grabens with up to 7 km of fill, which range in age from the Palaeogene to Pliocene (Lokichar, Lothidok, North Lokichar, North Kerio and Turkana Basins) (Fig. 2B). Two basins (Lokichar and Turkana) have been tested by two 3 km deep exploration wells operated by Shell Exploration and Production Kenya B.V. (Loperot-1 and Eliye Springs-1 wells), that demonstrated the existence of alternating thick packages of fluvial, fluvio-deltaic and lacustrine sediments (Morley et al., 1992, 1999b) (Figs. 1, 2B and C-1). In the central Kenya Rift, gravity, seismic reflection and magneto-telluric investigations have documented two 8 km-deep basins (Kerio and Baringo), that were probably initiated during Palaeogene time (Hautot et al., 2000; Mugisha et al., 1997) (Fig. 2B and C-2). Potential source rocks have been identified in the thick lacustrine strata of Oligocene or Miocene age that fill these basins. Reservoir quality rocks, mainly represented by arkosic grits, also occur in association with these potential source rocks (Morley et al., 1999b; Renaut, Ego, Tiercelin, Le Turdu, & Owen, 1999).

To the east of the Turkana Depression, extensive exploration by Chevron, Marathon, Mobil, Total, Amoco and Petrofina, together with their Kenyan partner NOCK (National Oil Corporation of Kenya), has concentrated on the NW–SE-trending Mesozoic–Cenozoic Anza Rift. This rift system extends to the southeast toward the Lamu embayment of southern Kenya and possibly links with the South Sudan Rifts to the north-west (Bosworth, 1992; Bosworth & Morley, 1994; Greene, Richards, & Johnson,

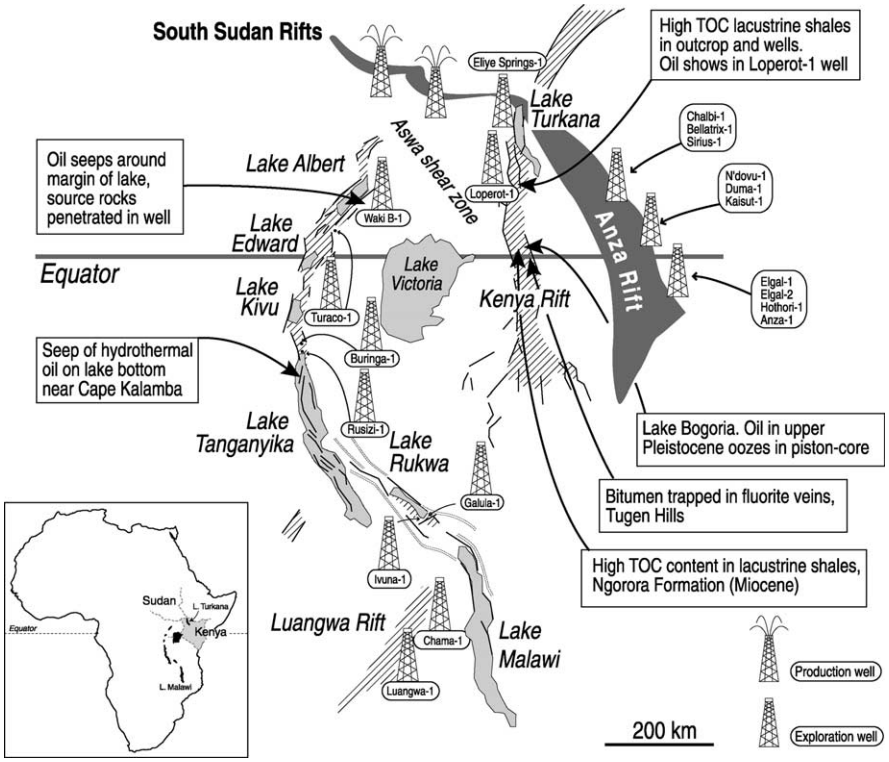

Fig. 1. Schematic map of the Central and Eastern African rift systems showing the main occurrences of potential source rocks and hydrocarbon seeps, and location of exploration/production wells drilled in Permo-Triassic, Cretaceous and Cenozoic rift basins in Central and East Africa (modified after Morley, 1999d).

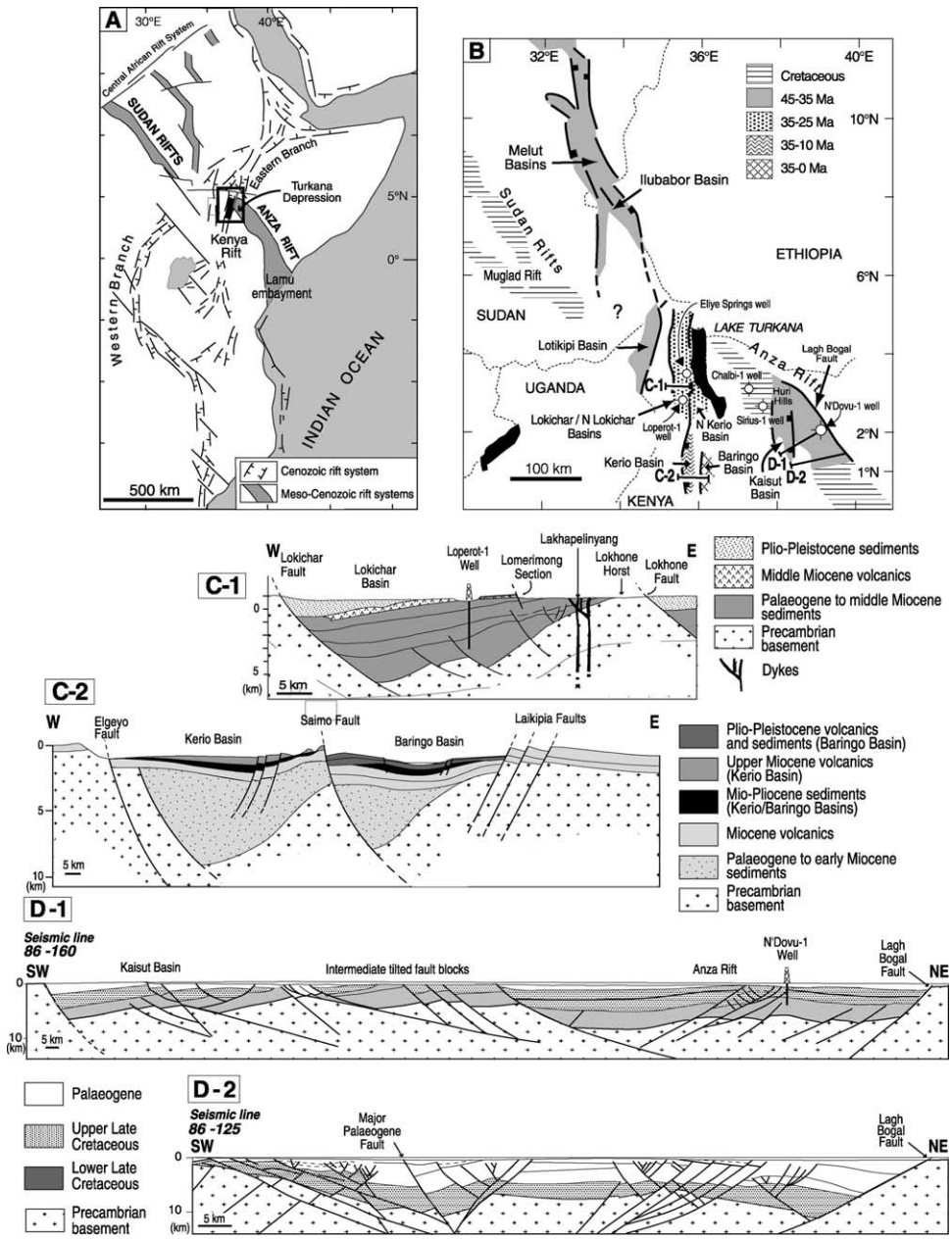

Fig. 2. (A) Location of the Turkana Depression, northern Kenya, within the Mesozoic and Cenozoic rift systems of Central and Eastern Africa (after Bosworth, 1992; Ebinger & Ibrahim, 1994). (B) Distribution map of the Cretaceous to Cenozoic rift basins in Sudan and northern-central Kenya (modified from Ebinger et al., 2000; Hautot et al., 2000; Morley et al., 1992). (C-1) Cross-section through the Lokichar Basin, southern Turkana. (C-2) Cross-section through the Kerio and Baringo Basins, central Kenya Rift (modified from Hautot et al., 2000). (D-1, D-2) Cross-sections through the Anza Rift (from Morley et al. (1999c)). See box (B) for location of the cross-sections.

1991; Morley et al., 1999c) (Figs. 1, 2A and B). This large multi-phase rift basin contains more than 6 km of syn-rift sediments of Mesozoic and Early Tertiary age (Winn, Steinmetz, & Kerekgyarto, 1993) (Fig. 2A, B, D-1 and D-2). It belongs, together with the southern Sudan rifts, to the Central African Rift System (CARS) (Fig. 2A and B) that formed synchronously with the breakup and separation of South America and Africa (Bosworth & Morley, 1994; Lambiase, 1989; Morley et al., 1999b; Schull, 1988). Extension and sediment deposition commenced in the Anza Rift during early Cretaceous time, while widespread rifting occurred during late Cretaceous. During the early Cenozoic, extension continued to affect the Anza Rift as well as parts of the Sudan rift system (Bosworth, 1992; Bosworth & Morley, 1994; Morley et al., 1992; Wescott, Morley, & Karanja, 1993) (Fig. 2D-1 and D-2). The Mesozoic rifts of Sudan have been demonstrated to be oil-rich (Mohamed, 2002; McHargue, Heidrick, & Livingston, 1992; Peterson, 1986; Schull, 1988).

Within the framework of a cooperative research program with the National Oil Corporation of Kenya in the Turkana Depression, two field campaigns (1997 and

1998) were conducted in order to examine the hydrocarbon potential of the Meso-Cenozoic structures, in terms of reservoir quality and also source-rock potential; the results of the latter are presented in a companion paper to the present work.

2. Regional stratigraphic background

The fluvial and fluvio-lacustrine clastic series that occur at different places in the Turkana Depression were originally named 'Turkana Grits' in the pioneer work of Arambourg (1933), Fuchs (1939) and Murray-Hughes (1933) (Fig. 3). These sequences of often immature clastics sometimes directly overlie the Precambrian basement, and were interpreted as either Mesozoic or Cenozoic deposits. In the Lapurr Range/Lokitaung Gorge at the northwest end of Lake Turkana (Fig. 3), dinosaur bones and angiosperm wood were found in a 400 m-thick series of arkosic sandstones and conglomerates (the Labur or Lubur series of Arambourg (1935)), suggesting a Cenomanian-basal Palaeocene age (Arambourg, 1943; Arambourg & Wolff, 1969; Fuchs, 1939; Williamson and Savage, 1986). Similar arkosic but often unfossiliferous sandstones are also known from discontinuous exposures on the southeast and west sides of Lake Turkana, in the Mount Porr area (Morley et al., 1992; Wescott et al., 1993; Williamson & Savage, 1986) and at the Lariu Range and Muruanachok, respectively (Walsh & Dodson, 1969; Wescott et al., 1993) (Fig. 3). Other basement-derived formations occur farther south of the Turkana area, in the Kerio and Baringo Basins (the Kimwarer and Kamego Formations) (Chapman, Lippard, & Martyn, 1978; Walsh, 1969) (Figs. 2B and 3). The latter two formations have been tentatively interpreted as linked to the first stages of rifting affecting central Kenya during the early Cenozoic (Hautot et al., 2000; Morley et al., 1992; Renaut et al., 1999). In other areas of the Turkana Depression (Lokichar, Lothidok, Nachukui) (Figs. 2B and 3), the 'Turkana Grits' contain a rich mammal fauna of Mio-Pliocene and Pleistocene age (Boschetto, 1988; Boschetto, Brown, & McDougall, 1992; Maglio, 1969; Mead, 1975), including hominid fossils and artifacts (Feibel, 1988; Feibel, Harris, & Brown, 1991; Roche et al., 1999). The use of the term Turkana Grits is now abandoned, and local formation names are used (Boschetto, 1988; Morley et al., 1992; Savage & Williamson, 1978). The available radiometric and biostratigraphic evidence indicates most of the sandstone complexes identified in the Turkana Depression can be related to either: (i) the system of N–S-trending half-grabens associated to the initial phases (Palaeogene to upper Miocene–Pliocene) of the East African rifting (Dunkelman et al., 1988; Morley et al., 1992) (Fig. 2B and C-1); or (ii) the Cretaceous–early Cenozoic Anza Rift (Figs. 2A, B, D-1, D-2, and 4).

In this paper, we present the results of a petrologic and diagenetic study that characterizes the origin and reservoir

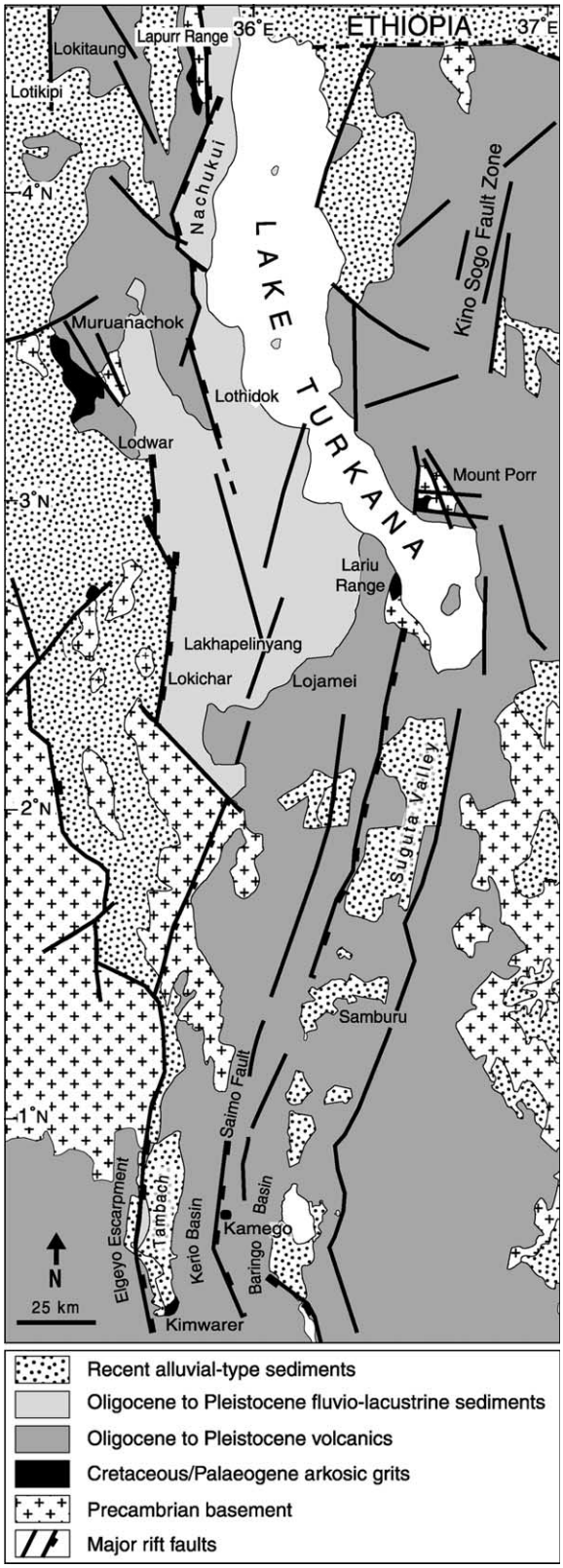

Fig. 3. Regional geology of the central and northern Kenya Rift showing the major rift faults and the metamorphic, volcanic and sedimentary terrains (compiled from Geological Map of Kenya, 1987; Joubert, 1966; Walsh, 1969; Walsh & Dodson, 1969).

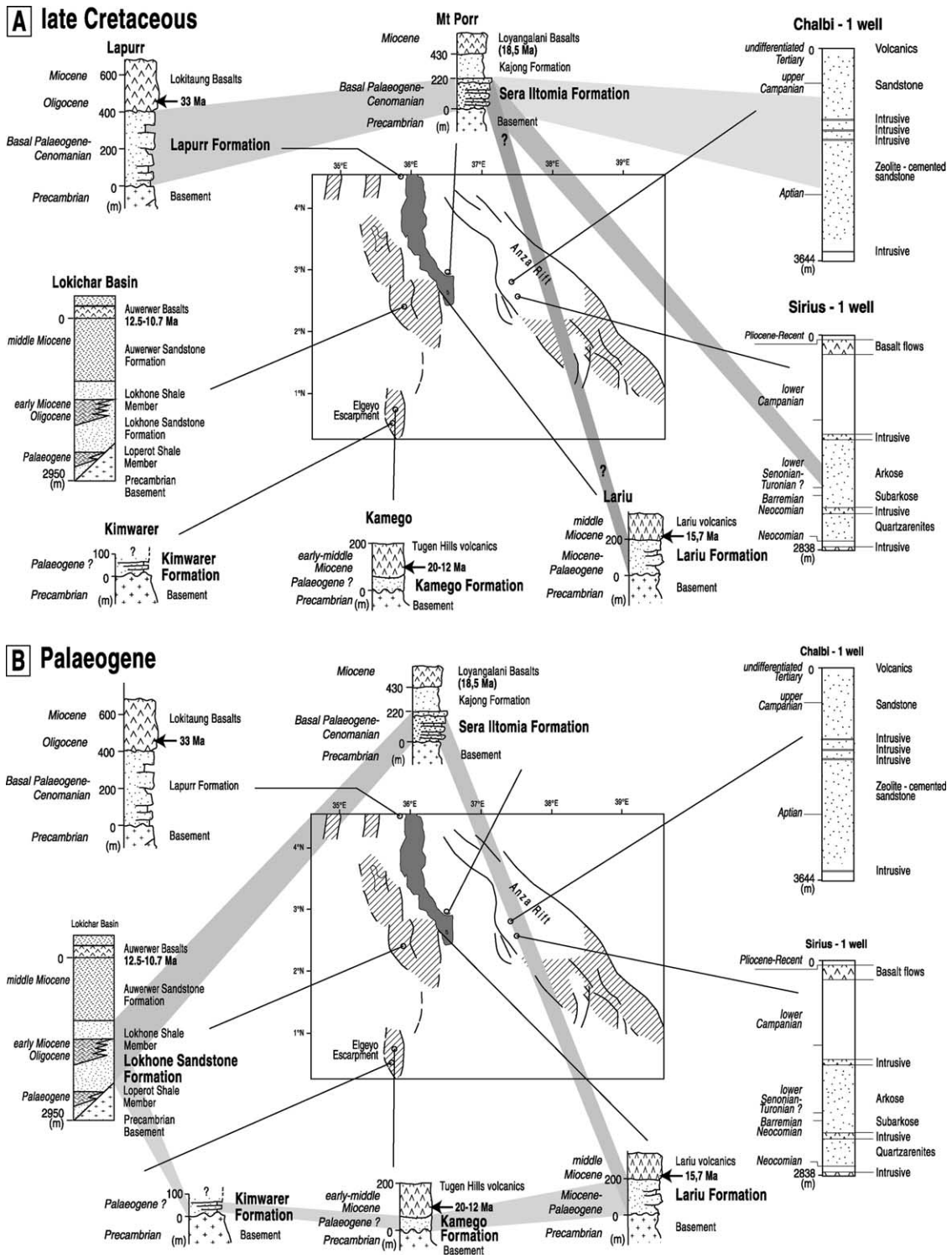

Fig. 4. Tentative correlation between the main arkosic sandstone formations cropping out in the Turkana Depression with the sandstones identified in the Chalbi-1 and Sirius-1 wells drilled in the Anza Rift (after Morley et al. (1999c)). (A) Late Cretaceous. (B) Palaeogene.

properties of two of the main grit series of the Turkana area: (i) the Auwerwer/Lomerimong Sandstone Formation in the Lokichar Basin (west Turkana) (Morley et al., 1999b); and (ii) the Sera Iltomia Formation in the Mount Porr Basin (southeast Turkana) (Savage & Williamson, 1978) (Fig. 3). A comparison between the different reservoir sandstones encountered in some of the wells drilled in the Anza Rift is also attempted (Fig. 4).

3. Reservoirs in the Lokichar Basin

3.1. Basin structure

The Lokichar Basin is a N–S-trending, Palaeogene half-graben 60 km long and 30 km wide (Morley et al., 1992, 1999b; Baker & Wohlenberg, 1971) (Fig. 2B and C-1). This first phase of the EARS rifting in northern Kenya occurred adjacent to an area of intense volcanism that commenced around 36 Ma in the Lotikipi region (Bellieni et al., 1981) and between 33 and 25 Ma in the Lokitaung region (Zanettin et al., 1983), followed by a more important

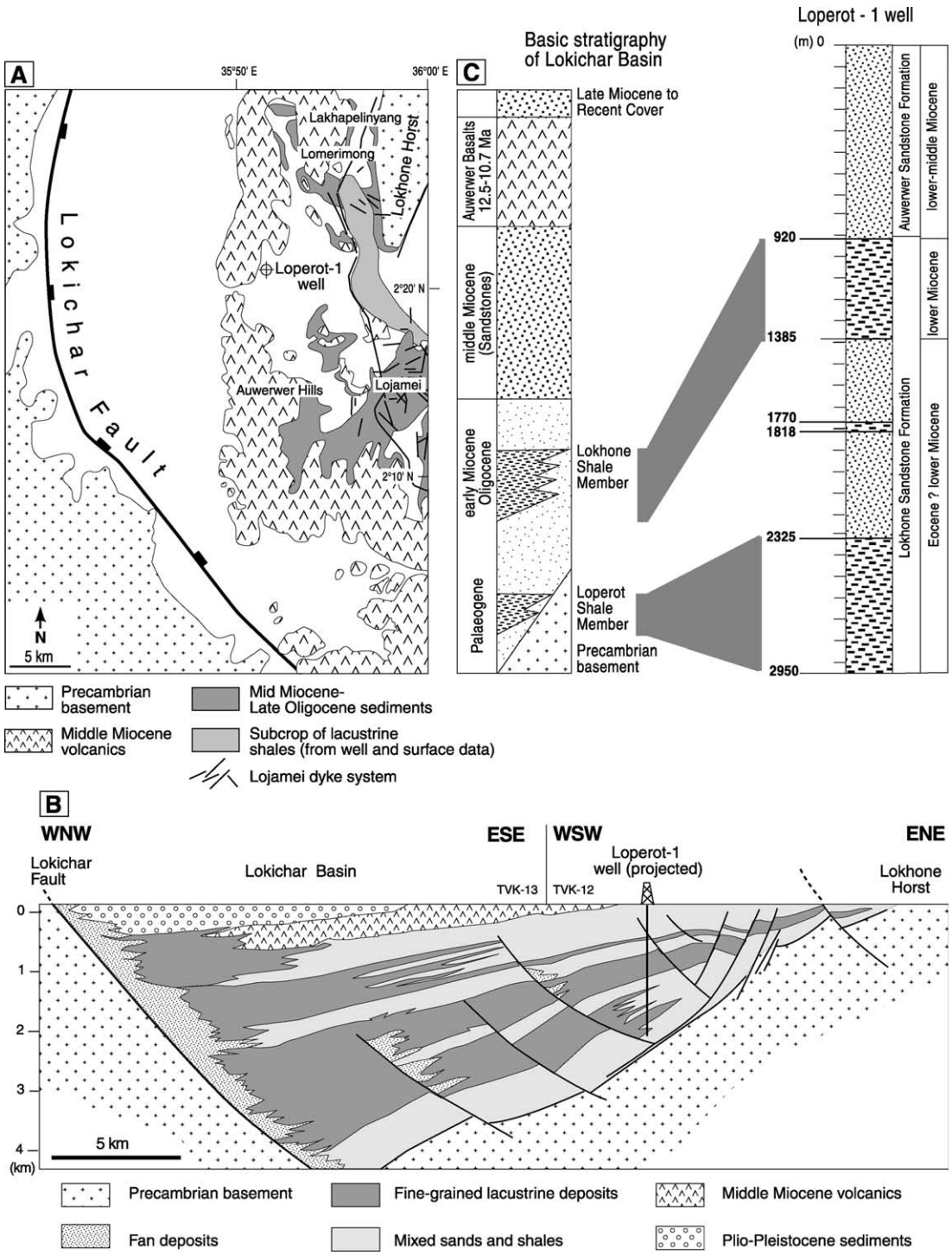

Fig. 5. (A) Schematic geological map of the Lokichar region (from Morley et al. (1999b)). (B) Composite dip cross-section across the Lokichar Basin, based on reflection seismic data (modified from Morley et al. (1999b)). (C) Basic stratigraphy of the Lokichar Basin and simplified lithostratigraphic colum of the Loperot-1 well (modified from Morley et al. (1999b)).

phase between 26 and 19 Ma in the area of Lodwar (Morley et al., 1999b; Zanettin et al., 1983) (Fig. 3). On industrial reflection seismic lines, the Lokichar Basin forms an east-facing half-graben floored by Precambrian crystalline basement and bounded to the west by a prominent east-dipping listric fault, the Lokichar Fault, with little or no present-day topographic expression (Morley et al., 1992, 1999b) (Fig. 5A and B). Its wedge-shaped sedimentary infill thickens dramatically to the west on top of Precambrian basement. As described by Morley et al. (1992, 1999b) and illustrated in Fig. 5B and C the fill is almost 7 km thick at its maximum and consists of Palaeogene to middle Miocene interbedded lacustrine and fluvio-lacustrine sediments. Capping the basin fill is a 300 m thick basaltic sequence with thin interbedded sediments, dated from 12.5 to 10.7 Ma and named the Auwerwer Basalts (Morley et al., 1999b).

The Lokichar area is also densely intruded by 2- to 10 m wide, N50° to N170°-trending igneous dykes, as are several other areas east and south of Lokichar (Lariu, Lojamei) and north of Lodwar (Dodson, 1971; Joubert, 1966; Wescott et al., 1993) (Figs. 3 and 5A). Some of these dykes were sampled during the 1998 field season in the Lokichar/Lojamei area. Two dykes, LOJ 01 (2 m-wide; N140° oriented) and LOJ 98-25 (5 m-wide; N50° oriented), are alkaline basalts. LOJ 20 (10 m-wide, N170° oriented) can be considered as a differentiated lava. They have been $^{40}K-^{40}Ar$ dated on whole rock fractions sized at 0.3–0.15 mm after crushing and sieving, and yielded ages between 17 and 13 Ma (Table 1). These ages are in the range of those presented by Morley et al. (1992) and Wescott et al. (1993) on the dyke system and lava flows of the Lariu Range area (Fig. 3). The basaltic dykes dated at around 17 Ma were emplaced during the major volcanic phase that affected the northern and central regions of the Kenya Rift (Samburu Basalts dated 23–16 Ma; Shackleton, 1946; Turkana Basalts dated 23–14 Ma; Baker, Mohr, & Williams, 1972; Joubert, 1966; Walsh & Dodson, 1969). Some of the other dykes were possibly injected contemporaneously with the Auwerwer Basalts at 12–10 Ma (Morley et al., 1992).

3.2. The Auwerwer/Lomerimong sandstone formation

The 7 km-thick basin infill of the Lokichar Basin has been partly calibrated by the ~3 km-deep Loperot-1 exploration well drilled in 1992 by Shell Exploration and Production Kenya B.V. (Morley et al., 1999b) (Fig. 5B and C). A possible late Eocene–early Oligocene age for the lowest sequence in the well is cited by Morley (1999b) This ~3 km-thick sediment pile includes alternating packages of coarse to fine sandstones tens to hundreds of meters thick, which from bottom to top are called the Lokhone and Auwerwer Sandstone Formations, respectively (Fig. 5C). The Lokhone Sandstone Formation includes two major shale intervals named the Loperot (lower) and Lokhone (upper) Shale Members, that are about 650 and 500 m thick in the Loperot-1 well (Morley et al., 1999b) (Fig. 5B and C). Exposures of the Lokhone and Auwerver Formations are poor, excepted to the north-north-east of Loperot, in the Lakhapelinyang area, where a 200 m thick grit sequence was described by Joubert (1966) and Boschetto (in Morley et al. (1999b)). In this study, a 100 m-thick section located at Lomerimong, 4 km south of Lakhapelinyang, has been investigated (Figs. 3 and 5A).

The Lomerimong section is part of the 200 m-thick Lakhapelinyang sequence. Through correlation of seismic reflection and well data to surface outcrops, this section corresponds to a part of the upper basin fill, represented by the Auwerwer Sandstone Formation (Figs. 5C, 6A and B). It lies close to the flexural margin outcrop of Precambrian basement (the Lokhone Horst) at lat 02° 27.575 N and long 35° 55.365 E (Fig. 5A). This area is dominated by a plateau several hundred meters high that provides almost continuous vertical sections. This plateau topography corresponds to the 300 m-thick Auwerwer Basalts (Morley et al., 1992), that dip gently to the west.

The lower half of the Lomerimong section is formed by 5- to 10 m-thick alternating beds of grey, green or brown red mudstones to siltstones and grey to beige coarse to pebbly sandstones. The upper half of the section comprises 3- to 6 m-thick beds of fine sandstones or clay-rich fine sandstones, which are grey, beige, yellow, red or purple in color. These sandstones and siltstones are generally massive or show locally horizontal and cross-bedding, whereas several beds of clay-rich fine sandstones are root-bearing (Fig. 6A).

3.3. Petrographic and diagenetic characteristics

Microscopic observations of sandstone/siltstone samples from the Lomerimong section show that, in addition to clay

Table 1
$^{40}K-^{40}Ar$ whole rock ages of Lojamei dykes, Lokichar Basin. Ages have been calculated following the constants recommended by Steiger and Jäger (1978), and errors in age at one sigma level have been quoted following Mahood and Drake (1982)

Sample	Analysis number	Average age (Ma)	Calculated age ± error (Ma)	$^{40}Ar^*$ (%)	$^{40}Ar^*/g$ (10^{-7} cm^3)	K_2O (wt %)	Weight (g)
LOJ 20	5944-8	12.9 ± 1.5	12.6 ± 1.0	11.9	5.675	1.39	0.7012
LOJ 20	5948-2		13.2 ± 1.5	8.6	5.925	1.39	0.3527
LOJ 98-25	5951-5		15.7 ± 0.8	18.1	5.487	1.08	0.5042
LOJ 01	5943-7	16.5 ± 0.4	16.2 ± 0.4	93.2	23.01	4.38	0.7046
LOJ 01	5950-4		16.9 ± 0.4	88.0	24.00	4.38	0.7019

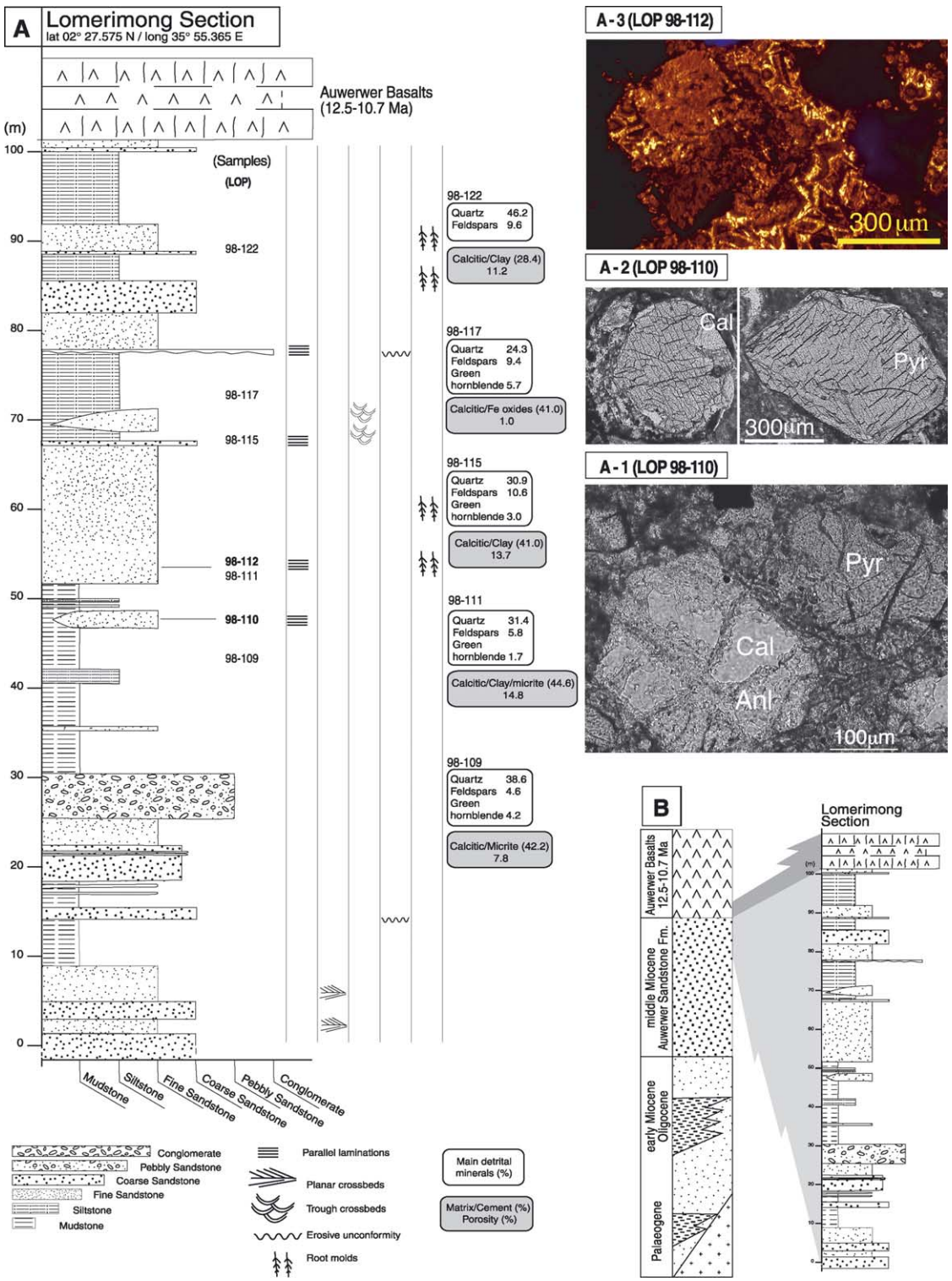

Fig. 6. (A) Sedimentary log of the Lomerimong section, Lokichar Basin: sedimentologic log. (A-1 and A-2) Detrital pyroxene phenocrysts, sample LOP 98-110. BW: black and white image; LP: plane polarized light; LPA: crossed polarized light. (A-1) Calcite–analcite pseudomorphs after pyroxene. Analcite forms microcrystalline ribbons which preserve the initial shape of the detrital minerals. Some of these microcrystal ribbons cross the pseudomorph from one side to the other. Calcite fills the pores remaining between the analcite ribbons (BW, LP images). (A-2) Preserved detrital pyroxene (right) and detrital pyroxene partially replaced by calcite (left). Cal: calcite; Anl: analcite; Pyr: pyroxene (BW, LP images). (A-3) Carbonate cement, sample LOP 98-112 (CL image). Generally the sandstones show homogeneous, orange-luminescent cement where the initial growth structures are not visible. However, in this sample, CL reveals evidence of a complex zonation pattern in the sparry calcite crystals. (B) Stratigraphic correlation between the Lomerimong section and the Auwerwer Sandstone Formation in the Lokichar Basin.

or micritic matrix (0–25%), carbonate cements (29–45%), detrital quartz (24–47%) and feldspar (6–11%), significant amounts of other detrital minerals are present: amphibole and pyroxene (0–6%), biotite (0–3%), muscovite (0–1%), and opaque minerals (1–15%). Tourmaline is also present in small amounts in some samples. Significant amounts of fresh volcaniclastic materials such as green or pale pink pleochroic pyroxene, green-brown pleochroic amphibole, plagioclase, opaques, as well as groundmass pebbles have been identified in the sandstones and siltstones at the bottom of the section (Fig. 6A; samples LOP 98-107 to 98-111). The volcanic component can reach more than 50% of the detrital material in some samples. Generally the phenocrysts are very well preserved, showing euhedral shapes. Microprobe analyses have been performed on the pyroxene and amphibole phenocrysts. The amphiboles are hornblendes of various compositions. The pyroxenes are calcium-rich diopside (Morimoto, 1988), suggesting a strongly undersaturated alkaline volcanic provenance (Vicat & Pouclet, 1995). Toward the top of the section, the volcanic component decreases, and quartz, K-feldspar, biotite and muscovite become progressively dominant, indicating a change in the sediment source.

In situ alteration of the volcanic material is characterised by the dissolution of the calcium-rich minerals (amphibole, pyroxene and plagioclase) and precipitation of pure sodium analcite and calcite (Fig. 6A; sample LOP 98-110). Some phenocrysts are completely or partially dissolved yielding secondary porosity, and commonly the latter was partially or completely filled by analcite and calcite. The first diagenetic phase to precipitate was euhedral analcite, which formed microcrystalline ribbons around or across the secondary pores that resulted from phenocryst dissolution. Typically, homogeneous calcite subsequently filled any remaining pore space (Fig. 6A-1) or partially replaced some phenocrysts (Fig. 6A-2). Analcite and calcite precipitated from Na/Ca-rich fluids related to the dissolution of the volcanic material. Indeed, the analcite–calcite pore filling is not observed at the top of the section where volcano-detritic material is absent. Further work is needed to constrain the origin of these fluid flow episodes but they are probably related to a thermal effect linked to regional volcanic activity.

A clay matrix (0–20%) or a micritic matrix (0–25%) also characterizes the Lomerimong sandstones. The detrital minerals show an angular shape. Polycrystalline quartz grains with deformation structures are locally present. There is no evidence of chemical burial diagenesis; for example, the feldspars are all well preserved. Early diagenesis is characterised by sparry calcite cements, which partially or completely fill primary porosity. We estimate an initial maximum primary porosity in the cemented zones of 40–45%, suggesting a very early cementation episode. Two main types of calcitic cements have been distinguished under cathodoluminescence (CL). Generally, the sandstones show homogeneous orange cement where the initial growth structures are not visible. However, in certain cases, CL reveals internally zoned sparite crystals (Fig. 6A-3; sample LOP 98-112). These crystals have a dog-tooth morphology, and are assumed to have grown inward from the wall of the pore toward its center. Under CL, the first growth zone is dark with a general evolution to vivid yellow zones in the pore center. Porosity estimates based upon point counting is rather low (1–15%) due to the abundance of calcite cement and micritic and/or clay matrix.

4. Reservoirs in the Mount Porr Basin

At the southeast end of Lake Turkana, in the Mount Porr-Kajong region, sedimentary strata consist mainly of fluvial siltstones, sandstones and minor conglomerates (von Höhnel et al., 1891) (Figs. 3, 7A–C). They comprise two major sedimentary formations, the lower 'Sera Iltomia Formation' (220 m thick) (Fig. 8A), and the upper 'Kajong Formation' (200 m thick) (Savage & Williamson, 1978). Both unconformably overlie crystalline basement rocks (mainly gneisses and amphibolites) of Proterozoic age, and are in turn overlain by lower Miocene sediments and basalts (dated at 18.5 ± 0.45 Ma) forming the Loiyangalani Formation, and by Pliocene basalts dated at 3.38 ± 0.25 Ma, respectively (Williamson & Savage, 1986). On the basis of the lack of any volcaniclastic component in the Sera Iltomia sandstones and the discovery of angiosperm fossil wood, a late Mesozoic–basal Palaeocene age is proposed for the Sera Iltomia Formation (Savage & Williamson, 1978; Williamson & Savage, 1986).

4.1. Basin structure

The structure of the Mount Porr-Kajong area is dominated by a regional normal fault pattern striking at N160° and by fewer but significant N90°- and N60°-striking transverse faults that also show prominent normal displacements. The sedimentary deposits of the Sera Iltomia and Kajong Formations are mainly exposed in a triangular-shaped lowland that is separated from a crystalline basement high to the north by two major N90°-striking structures identified as the Kajong lineaments by Savage and Williamson (1978) (Fig. 7A and B). The main Kajong lineament is topographically expressed by a 10 km-long escarpment that has been defined as the Kajong Fault Zone (KFZ) while the Mount Porr Fault Zone (MFZ) exhibits a weaker morphological expression (Fig. 7B and C). Near the western end of KFZ, a small basanitic intrusion has been identified close to the fault zone while, near the eastern end of KFZ, a dense set of south-dipping extensional faults are intruded by a few dm-thick mugearitic dykes with an approximate N90° trend (Fig. 7B and C). Such N90°-trending faulted structures are quite atypical in the EARS. They have been identified in the southern Sudan rifts (Bosworth, 1992) and in southern Ethiopia, where N90°-striking Cretaceous dykes and

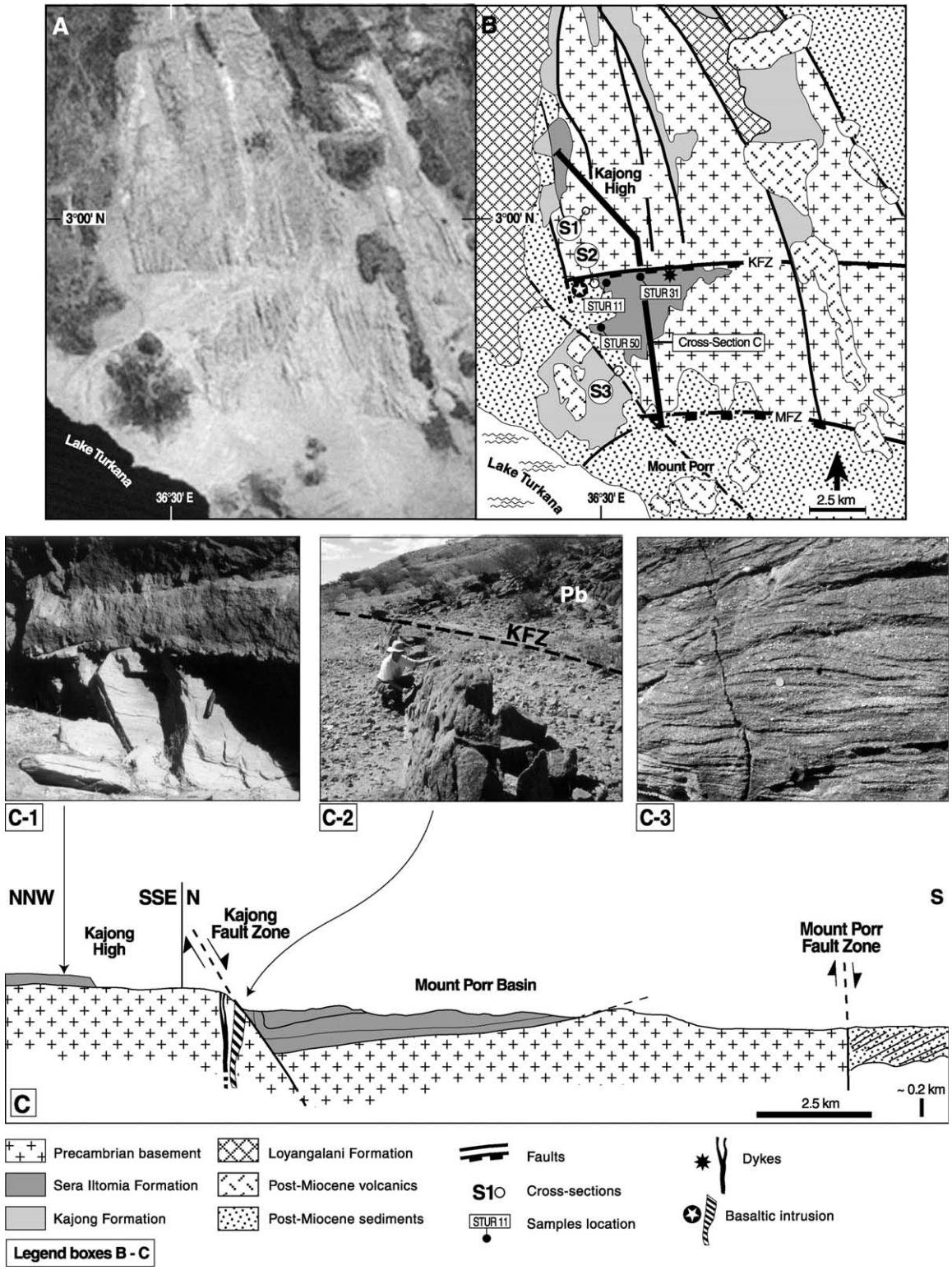

Fig. 7. (A) Satellite imagery (from Landsat MSS 5; Mount Kulal, Kenya). (B) Geological map of the Mount Porr-Kajong area, south-east Turkana (modified from Williamson and Savage (1986)). (C) Composite geological cross-section through the Kajong High, the KFZ and the Mount Porr Basin showing the intrusive volcanics along the faulted zone and the vertical attitude of the Sera Iltomia beds on the immediate hanging wall of the KFZ. (C-1) Nearly horizontal contact between the Precambrian basement (amphibolites) and coarse-grained sandstones of the Sera Iltomia Formation at latitude 03° 00.390 N and longitude 36° 29.954 E, KFZ footwall. (C-2) Coarse-grained sandstone beds dipping 75° to the south on the immediate hanging wall of the Kajong Fault Zone (KFZ). Pb: Precambrian basement; dotted line: trace of the KFZ. (C-3) Coarse-grained sandstone with wide trough crossbeds, representative of a braided river system (2 cm diameter coin for scale).

strike-slip faults have been described (Ebinger & Ibrahim, 1994). On the western side of Lake Turkana, in the Lodwar area (Fig. 3), N90°-trending faulted structures are evidenced by drainage network diversion (Vétel, Le Gall, Tiercelin, Johnson, & Collet, submitted for publication).

From field and cartographic evidence, the composite Kajong fault network appears to be capped by the Loiyangalani Basalts and thus assumed to be pre-lower Miocene in age (Williamson & Savage, 1986) (Fig. 7B). The precise age of faulting cannot be directly defined, however, and its attribution to either the early Cenozoic or Cretaceous rifting events depends mainly upon the age assigned to: (1) the sediments involved in the faults (Sera Iltomia and Kajong Formations), and (2) the syn-extensional basanitic intrusion and dm-thick mugearitic dykes injected along the KFZ at its westernmost (lat 02° 58.523 N; long 36° 30.008 E) and easternmost (lat 02° 58.620 N; long 36° 31.410 E) tip zones, respectively (Fig. 7C). Unfortunately these mugearitic dykes as well as the basanitic intrusion are strongly altered (possible hydrothermal alteration), and cannot be isotopically dated. However, they can be tentatively correlated on the basis of their petrography with the dyke systems identified immediately west of Lake Turkana, in the Lariu and Lokichar/Lojamei areas (Figs. 3 and 5A), that have an age of about 16–17 Ma (Joubert, 1966; Morley et al., 1992; Wescott et al., 1993; this work). These fault-intrusion relationships could testify to activity of E–W-striking normal faulting and coeval fissural volcanism in the Mount Porr area, contemporaneous with the Loyangalani basaltic volcanism during lower-middle Miocene.

4.2. The Sera Iltomia formation

The isolated exposures of sedimentary rocks belonging to the Sera Iltomia Formation probably represent dismembered parts of a single basin, the so-called Mount Porr Basin, which formed upon Proterozoic basement, and was subsequently disrupted by successive episodes of faulting. The sediments are commonly in faulted contact with the Proterozoic basement, but stratigraphic basement/grit contacts are locally preserved, such as the nearly horizontal unconformity observed on the footwall of the KFZ (Figs. 7C-1 and 8B; section 1 at lat 03° 00.390 N and long 36° 29.954 E), and the angular unconformity located on the KFZ hanging wall (lat 02° 56.342 N and long 36° 30.864 E; Figs. 7B and 9A-1; section 3). The Sera Iltomia Formation is divided into four main members that comprise a variegated succession of conglomerates, medium to coarse sandstones and fine sands, silts and silty mudstones (Fig. 8A). During two successive field seasons in the Mount Porr area, several sections were studied and sampled on both the footwall and hanging wall of the KFZ (Figs. 8B, C and 9).

On the KFZ footwall, up to 20 m-thick yellow-brown medium to coarse sandstones rest horizontally on an amphibolitic basement, with a clean and scoured surface overlain by quartz gravels and pebbles, and locally dm-sized clasts of basement (Figs. 7C-1 and 8B; section 1). These sandstones are horizontally stratified or locally show planar-crossbed sets or trough crossbeds (Fig. 7C-3). To the south, on the immediate hanging wall of the KFZ, reddish-brown, 10 m-thick well-bedded coarse sandstones with numerous scattered quartz granules and pebbles alternate with fine-grained sandstones and a few conglomeratic beds. There, the beds lie in a nearly vertical (75°) position at N90°E (Figs. 7C-2 and C-3; 8C and C-1; section 2). The sandstones are composed of sub-rounded quartz grains (45–80%) with small (1 mm) single-crystal grains and larger (several mm) polycrystalline grains, and feldspars (5–25%), predominantly microcline (Fig. 8C; sample STUR 06). At the eastern tip of the KFZ, well-bedded fine to very coarse, almost structureless sandstones (up to 45 m thick) with scattered sub-rounded quartz grains and pebbles, form beds that dip 54° toward the southeast, and which are separated from the basement by fault breccia several meters thick.

To the south, on the distal part of the KFZ hanging wall, alternating beds of medium to coarse sandstone and silty mudstone dip northward at 15–25° N, forming a 290 m-thick section (location: lat 02° 56.219 N and long 36° 30.711 E) (Fig. 9A, section 3). This section is the most complete within the Sera Iltomia Formation in this area, and possibly represents Member 4 of Williamson & Savage (1986) (Fig. 8A). It consists of alternations of 1- to 3 m-thick beds of white, grey or yellow medium to coarse-grained pebbly sandstones and 4-to 20 m-thick beds of beige-green silty mudstones, capped by red and white sandstone and mudstone beds. The sandstone beds are generally massive with a flat base and top. Locally, they show flat-bedding and planar crossbed sets, and only a few beds exhibit an erosive base. In addition, this section shows clear evidence for inversion tectonics as expressed by large wavelength upright folding and related reverse faults (Fig. 9A-1). Such compressive tectonics have been described in other regions of the Turkana Depression as well as in the Anza and Sudan Rifts and other segments of the East African Rift System (Lake Rukwa Rift) (Fig. 1). They have been interpreted as being Plio-Pleistocene and Holocene in age in the Turkana area, and of Palaeogene age in the Anza and Sudan Rifts (Bosworth, 1992; Bosworth & Morley, 1994; Guiraud & Bosworth, 1997; Morley et al., 1999c).

4.3. Petrographic and diagenetic characteristics

In the Sera Iltomia sandstones, the main detrital minerals are quartz (40–70%) and feldspars (microcline or plagioclase, albite to oligoclase) (5–25%) (Figs. 8B, C and 9A). Interstitial clay and oxides form up to 7–36% of the whole rock. The quartz fraction consists mainly of small (1 mm) sub-rounded, single-crystal grains and larger (several mm) polycrystalline grains that exhibit deformational features such as undulatory extinction and polygonal recrystallization (Fig. 8B-1; sample STUR 98-12). Detrital feldspars are

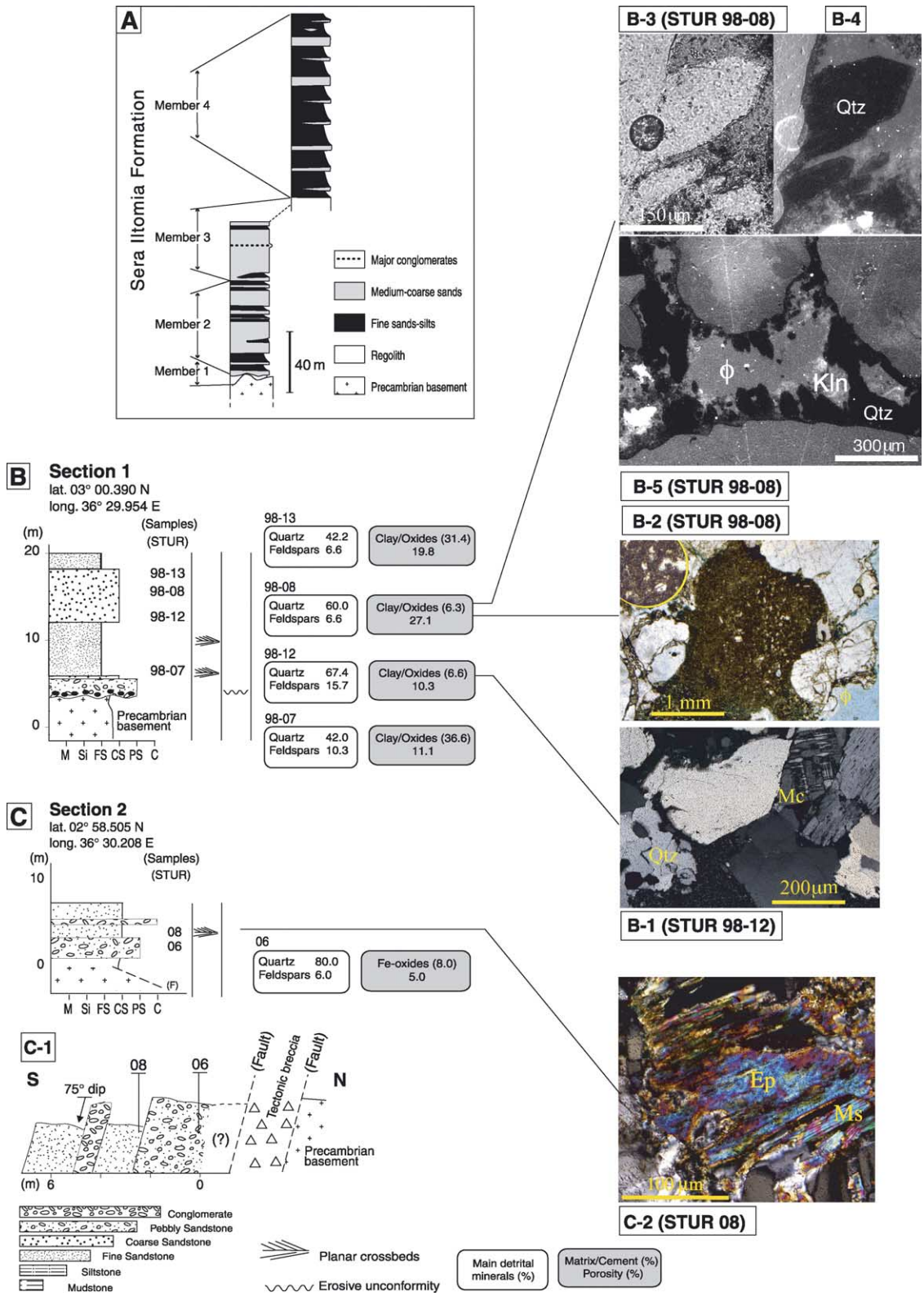

Fig. 8. (A) Generalized stratigraphic section of the Sera Iltomia Formation (from Williamson and Savage, 1986). (B) Sedimentary log (Section 1) measured in the field through the Sera Iltomia Formation in the footwall (B) of the Kajong Fault Zone (for the location of section, see Fig. 7B). (B-1) Common detrital minerals from the Mount Porr series are microcline (Mc) and strained quartz (Qtz) grains suggesting a mainly metamorphic source. Sample STUR 98-12; LPA image. (B-2) Clay matrix between angular detrital quartz grains. Here the clay matrix contains small detrital grains of quartz and micas. The circle shows a detail of the clay matrix. Φ: Porosity. Sample STUR 98-08; LP image. (B-3 to -5) Black and white optical microphotographs of quartz overgrowths in the STUR 98-08 sandstone (LPA images). (B-3) Detail of euhedral quartz crystals growing on a detrital grain (LP image). (B-4) Quartz overgrowth is non-luminescent (completely black) under cathodoluminescence. (B-5) General view of quartz overgrowths in a pore (CL image). The two types of quartz

generally well preserved, but locally exhibit minor alteration to sericite due to weathering and dissolution related to calcite cementation. Feldspar and quartz grains also show recrystallization textures. The feldspar composition, the textures of quartz and feldspar grains, and the presence of tourmaline inclusions in quartz and epidote pseudomorphs after muscovite suggest that regional metamorphic rocks were the primary provenance of the studied sandstones (Fig. 8C-2; sample STUR 08).

The other detrital constituents of the Sera Iltomia sandstones are a muddy matrix and carbonate ooids. The muddy matrix consists of clay minerals, and locally contains small grains of quartz and mica (Fig. 8B-2; sample STUR 98-08). The clay matrix exhibits show flow textures when it is indented or compacted between detrital grains. These observations suggest that the clay matrix may in part be derived from mud clasts which suffered compaction and recrystallization after deposition. Carbonate ooids (Fig. 9A-2; sample STUR 98-40) are a minor constituent of some sandstones (<5%). They could be of bacterial origin (Reid, Macintyre, & Post, 1992) and can act as a nucleus for carbonate cements. The detrital grains are generally unaltered showing no evidence of burial diagenesis. Nevertheless, different early diagenesis events are recorded in a few samples by carbonate, quartz or kaolin cements (Figs. 8D-3 and 10A–C). Some very rare relic euhedral rhombohedral dolomite crystals are present in a few sandstones (Fig. 9A-3; sample STUR 98-42). These crystals are pseudomorphed by calcite and iron oxides. Such dedolomitisation may be evidence of a meteoric fluid flow episode.

Quartz overgrowths and quartz cement have been found in two samples, STUR 98-08 (Fig. 8B-3–5), and STUR 31 (Figs. 7B and 10A). The first sample (STUR 98-08) is a poorly sorted sandstone (60% quartz) with a minor clay matrix content (6%). Two types of quartz syntaxial overgrowths have been observed under CL microscopy (Fig. 8B-3–5): (i) quartz rims of variable thickness around detrital quartz grains, and (ii) small euhedral quartz crystals which develop in optical continuity with the detrital quartz. A few fluid or solid inclusions were found at the limit between the overgrowths and the detrital core. Generally, the overgrowths show undulatory extinction in optical continuity with the detrital core. Some pores with quartz overgrowths are completely filled by clay cement. At high magnification, this cement appears to consist mainly of micrometric vermiform kaolin crystals. The porosity is rather high (20–25%). There is no evidence of pressure solution structures such as sutured contacts between quartz grains. In addition, there is no evidence of local dissolution of minerals which could have acted as a silica source for the quartz overgrowths. The non-luminescent nature of the quartz under CL (i.e. completely black) (Fig. 8B-3–5) indicates its precipitation from a silica-saturated fluid at low temperature (Marshall, 1988). Moreover, the total absence of zonation suggests a single fluid–rock interaction episode with a very homogeneous fluid composition. The second sample (STUR 31) is a calcite-cemented sandstone (Fig. 10A). The detrital grains are quartz, K-feldspar and plagioclase and the intergranular porosity is completely occluded by calcite cement (40%). A small irregular zone of the thin section (2 mm in diameter) contains detrital minerals (e.g. strained quartz, plagioclase and microcline), completely cemented by quartz. This quartz cement, which is non-luminescent, shows homogenous extinction under the polarising microscope. The proportion of the quartz cement in the zone is about 40%, but the relationships between calcite and quartz cements are unclear, although the former seems to have precipitated after the quartz cement.

CL reveals five successive calcite cementation phases (Fig. 10D–F). The cement content is highly variable (0–42%). Exsolution of oxides showing calcite recrystallization is common although the sandstones contain no evidence of an internal source of calcium and carbonate ions for the calcite cementation. For instance, plagioclase grains are generally well preserved with only minor dissolution marks. The sparitic texture of the cements and their bright yellow-orange colors in CL suggest a meteoric fluid flow origin for these cements. On the other hand, the iron oxide exsolution during dolomite dissolution or calcite recrystallization suggests an episode of oxidising fluid flow. Kaolin has been observed in a few samples, STUR 98-08 (Fig. 8B, section 1) and STUR 11 and 50 (Fig. 7B). Kaolin was precipitated in porosity remaining after quartz overgrowth development (Fig. 8B-3–5) or after calcite cementation (Fig. 10B; sample STUR 50). Its development was not related to local alteration of feldspar grains. Alteration of muscovite to kaolin is very rare (Fig. 10C; sample STUR 11), but in such cases, kaolin replaces muscovite along its cleavage planes and the kaolin crystals (Kln) also form clusters in the surrounding porosity. In the calcite-cemented sandstones, kaolin forms clusters of small crystals (20 μm) in open pores between detrital grains (Fig. 10A). The relative timing of kaolin precipitation is revealed by its relationships with the calcite cementation phases: it formed after the (a) phase and before the (c) phase (Fig. 10G). In the STUR 98-08 sandstone (Fig. 8B-2, section 1), kaolin developed after quartz overgrowth as 1–2 μm long

overgrowths are shown. A quartz rim around the detrital grain. Small euhedral and elongated grain growing from the detrital core. Kaolin crystals (Kln) either partially or completely fill the remaining pore space. Φ: Porosity. (C) Sedimentary log (Section 2) and corresponding cross-section measured through the Sera Iltomia Formation in the hanging wall of the Kajong Fault Zone (see Fig. 7B for location of section). (C-1) Cross-section 2 showing steeping inclined (75°), E–W striking coarse sandstones alternating with fine-grained sandstones and a few conglomeratic beds. The faulted contact between the sandstones and the basement is underlined by a several m-thick zone of tectonic breccia (see Fig. 7C-2). (C-2) Pseudomorph of epidote (Ep) after muscovite (Ms). Sample STUR 08; LPA image.

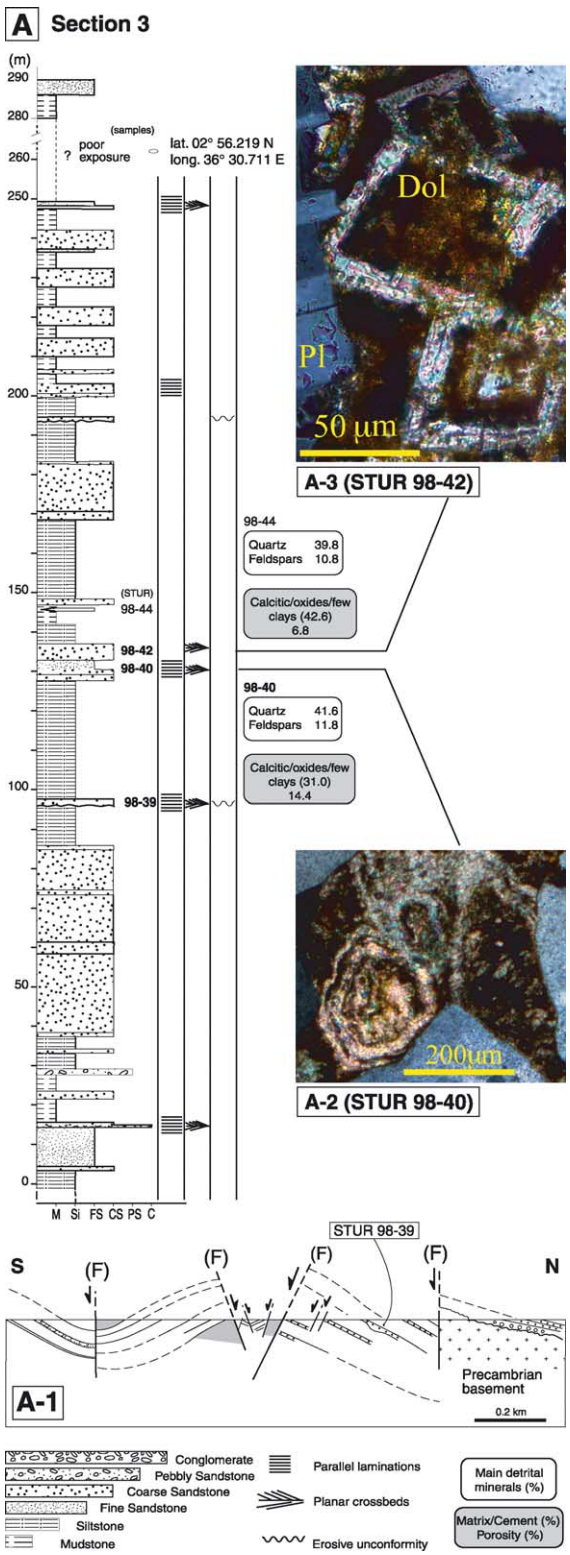

Fig. 9. (A) Sedimentary log and corresponding cross-section of Section 3 measured through the Sera Iltomia Formation in the hanging wall of the Kajong Fault Zone (KFZ) (see Fig. 7B for location of section). (A-1) Section 3 shows clear evidence for inversion tectonics, consisting of broad upright syncline-anticline pair with a wavelength of about 500 m and trending nearly at N70°, subsequently disrupted by normal faulting. (A-2) Carbonate ooids are a minor constituent of some sandstones. Sample STUR 98-40, LPA image. They commonly act as nucleus for carbonate cements. (A-3) Calcite-iron oxide pseudomorphs after dolomite (Dol). The initial rhombohedral crystal shape of dolomite is still visible and is now occupied by calcite and iron oxides. The blurred outlines of the initial dolomite rhombs suggest a volume increase during the dolomite replacement by calcite. Pl: Plagioclase. Sample STUR 98-42, LPA image.

vermiform ribbons which fill the pores. The kaolin group comprises three polytypes with the same composition, kaolinite, dickite, and nacrite (Buatier, Potdevin, Lopez, & Petit, 1996). Identification of the kaolin polytypes can be achieved by X-ray diffraction or infrared spectroscopy, but the quantity of kaolin in the studied samples is, unfortunately, insufficient to perform such analyses. Nevertheless, based on their morphology, the kaolin crystals could be kaolinite. Indeed, cluster or vermiform kaolinite is the common form of diagenetic kaolin in sandstones (Hassouta, Buatier, Potdevin, & Liewig, 1999). Whatever the exact polytype, the precipitation of kaolin in open pores and the preservation of the aluminous detrital minerals both indicate an episode of an aluminous-rich fluid flow through the sandstones. The chronology of the different early diagenetic events which affect the Sera Iltomia sandstones are summarised in Fig. 11.

Porosity estimates based upon point counting range from 1 to 33%. Low porosities result from a higher clay matrix content (up to 35%) or from a higher calcite cement content (up to 42%). In the first case, the initial porosity was lower due to primary accumulation of clays and mud clasts. Furthermore, a high initial clay content allows porosity reduction by compaction and deformation of the clay matrix. In the second case, the initial porosity was higher and porosity reduction occurred by calcite precipitation. However, cementation limits mechanical deformation and the remaining porosity can then be preserved. The carbonate cements are heterogeneously distributed in the studied sandstones, and no evidence for a lithological control of the cementation has been found.

5. Depositional settings, fluid–rock interaction and diagenesis

The two sandstone formations studied here, the Auwerwer/Lomerimong sandstone succession in the Lokichar Basin, and the Sera Iltomia Formation in the Mount Porr Basin, have developed in structural settings formed during two major successive phases of rifting that affected central and eastern Africa. The Auwerwer/Lomerimong sandstones are clearly linked to the Palaeogene–middle Miocene rift phase that corresponds to the first episode of the EARS in central-northern Kenya and southern Ethiopia (Ebinger et al., 2000; Hautot et al., 2000; Morley et al., 1992) (Fig. 2B). The poorly dated Sera Iltomia Formation can be interpreted either as linked to the Mesozoic–early Cenozoic Anza/South Sudan rift system, or to the first EARS episode

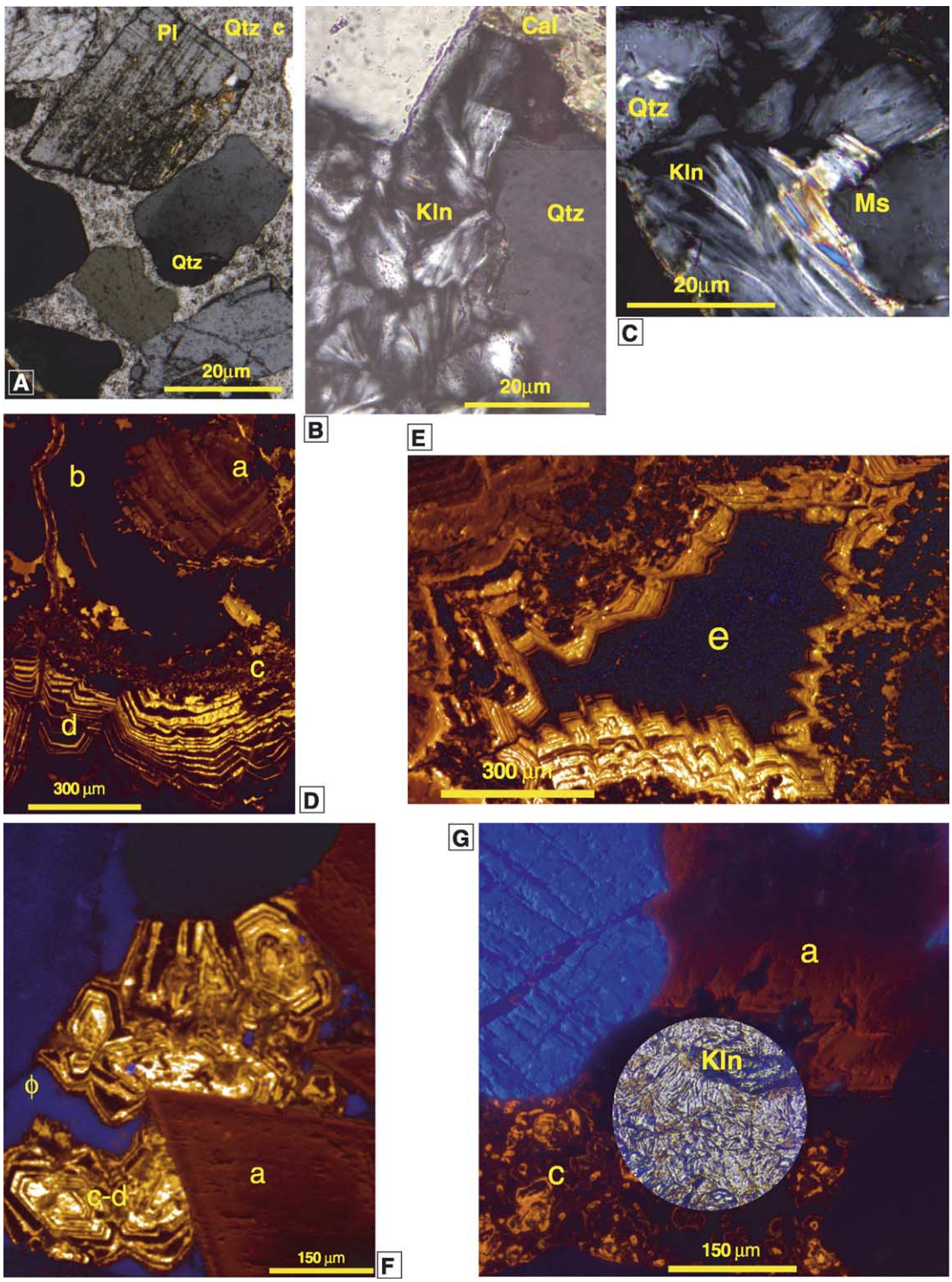

Fig. 10. (A) Quartz cement (Qtz c) filling the porosity. Pl: Plagioclase. Sample STUR 31; LPA image (see Fig. 7B for sample location). (B) Cluster of authigenic kaolin crystals (Kln). The kaolin crystals (Kln) and calcite (Cal) fill the pores between detrital quartz (Qtz) grains. Sample STUR 50; LPA image. (C) Alteration of muscovite (Ms) to kaolin. Sample STUR 11; LPA image. The kaolin crystals (Kln) form clusters adjacent to the mica. Kaolin also replaces the mica along its cleavage planes. Qtz: quartz. (D) to (G) Cathodoluminescence (CL) microphotographs of carbonate and kaolin cements. (A) Calcite pore filling showing four successive cementation phases (a, b, c, d) (sample STUR 98-11; Fig. 7B, section 1). Phase (a) consists of sparitic grains up to 0.5 mm in diameter with a brown to dark orange color in CL. A non-luminescent CL rim of calcite (phase b) follows phase (a). Phase (c) consists of small (<10 µm) euhedral calcite grains showing alternating black, orange or yellow growth zones. Phase (d) shows a sparitic texture with oscillatory zoning revealed by alternating black-yellow growth zones. (B) Calcite pore filling (sample STUR 98-11) showing the (a) to (d) phases. A fifth cement (e) fills the remaining porosity. (C) Calcite cement relationships (sample STUR 11; Fig. 7B). The five calcite phases are rarely present together. This image shows clearly that the (c)–(d) phases post-date the (a) phase. Φ: Porosity. (D) Kaolin and calcite cement relationships (sample STUR 11; Fig. 7B). Clusters of kaolin crystals (Kln) (circle with polarised light) and two calcite cements similar to the (a) and (c) phases fill the porosity. Kaolin precipitation occurred after phase (a) but before phase (c).

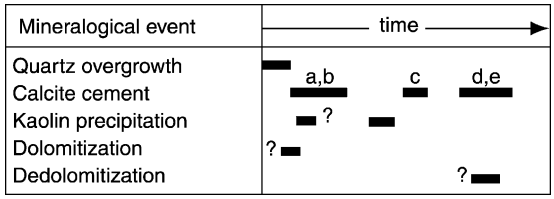

Fig. 11. Schematic diagram giving the relative chronology of the different early diagenetic phases observed in the sandstones of the Sera Iltomia Formation. Letters a, b, c, d and e refer to the different calcite cements shown on Fig. 10D–G.

in northern Kenya, but prior to any phase of volcanic activity.

5.1. The Auwerwer/Lomerimong sandstone formation

The lower-middle Miocene Auwerwer/Lomerimong sandstone succession documents two distinct sources for the clastic material. A volcanic source is apparent in the lower part of the studied section. The influence of this source progressively decreases toward the upper part of the section, where it is replaced by a basement-linked source. The detrital minerals associated with the volcanic source (diopside and amphibole phenocrysts, feldspathic mesostase) reflects alkaline volcanism. Further, these deposits exhibit palaeocurrent directions to the west, north and east, suggesting a generally northerly directed flow (Morley et al., 1992, 1999b). The basaltic flows and tuffs of the Samburu Basalts Formation that started to erupt at around 23 Ma to the south and southeast of the Lokichar Basin (Baker et al., 1972; Chapman & Brook, 1978; Dunkley, Smith, Allen, & Darling, 1993; Golden, 1978; Shackleton, 1946) (Fig. 3) could represent this volcanic source. This would suggest a major axial drainage system issued from the regions located south of the Lokichar half-graben and fed fluvio-deltaic complexes that developed at the southern end of the basin. Nevertheless, the excellent preservation of pyroxene phenocrysts in several beds of the Lomerimong succession also suggests that the source of some of the volcanic material was close to the deposition site, possibly less than 50 km, and that no or very little fluvial transport was involved. Such crystals may have issued from nearby explosive volcanic centres, and were rapidly incorporated at the depositional site.

At the top of the Auwerwer/Lomerimong series, the basement-derived products have a low biotite and muscovite content, and no deformation structures in the quartz grains. This suggest a source other than the gneissic complexes of the Mozambique Orogenic Belt which lie southeast of the Lokichar area (Hackman, 1988). These products may originate from granitic basement exposed south-southwest of the Lokichar Basin and as far as the central part of the Kenya Rift (Kerio-Baringo Basins) (Key, 1987; Smith & Mosley, 1993), where similar arkosic facies are known from the Palaeogene old Kimwarer and Kamego Formations and the lower Miocene Tambach Formation (Chapman et al., 1978; Renaut et al., 1999; Walsh, 1969) (Fig. 3). In terms of diagenesis, intense dissolution of detrital volcanic minerals in the Auwerwer/Lomerimong sandstones has promoted secondary porosity formation. Nevertheless, calcite–analcite precipitation, possibly in association with hydrothermal fluid circulation linked to tectonic/volcanic activity. Such hydrothermal circulation could relate to the emplacement of the Loperot and Lojamei dyke swarms at 17 and 12 Ma. Widespread calcite cementation during early diagenesis significantly reduced the porosity which ranges between 0 and 15%, resulting in a poor reservoir quality.

5.2. The Sera Iltomia sandstones

The sedimentary facies observed on the footwall and immediate hanging wall of the KFZ suggest high-energy braided stream conditions (Member 3 of Williamson and Savage (1986)) while the channel and overbank facies (Member 4 of Williamson and Savage (1986)) indicates the deposition in a non-braided fluvial system. The main detrital minerals identified in the Sera Iltomia sandstones are all immature and strictly basement-derived. Typical metamorphic textures identified in quartz, microcline and biotite grains suggest a regional metamorphic rock origin. The few palaeocurrent directions indicate sediment transport in a broadly NNW to NE direction, indicating an aggrading fluvial surface that completely buried the underlying basement (Williamson & Savage, 1986; Wescott et al., 1993). Such data suggest a sediment source from a basement area south of Lake Turkana. Considering the possibility of a Palaeocene age for the Sera Iltomia Formation, sedimentation can be related to the system of N–S oriented basins initiated during the early Cenozoic phase of EARS rifting in northern Kenya, as is also suspected for the nearby undated Lariu arkosic grits, visible on the southwest shore of Lake Turkana (Wescott et al., 1993) (Fig. 3). Both the Sera Iltomia and Lariu Formations may correspond to the Palaeogene–early Miocene section observed on seismic lines forming the base of the Lokichar Basin infill. They may also be related to the Kimwarer and Kamego arkosic formations in central Kenya Rift (Morley et al., 1999b; Wescott et al., 1993) (Fig. 3).

Immature red-colored arkosic sandstones similar to the Sera Iltomia sandstones, and associated with lacustrine shales, have been encountered in wells drilled in the central and southeastern regions of the Anza Rift (Fig. 4). Such sediments range from Cenomanian to Campanian in age and indicate fluvial input of clastics from the northwest along the N140°-trending axis of the Anza Rift, possibly associated with basement uplift in southern Sudan and Ethiopia that was active during different pulses of rifting that characterize the Anza Rift (Bosworth & Morley, 1994; Winn et al., 1993). To the northwest of the Turkana Basin, in the area of the Lapurr Range/Lokitaung Gorge (Fig. 3),

the Cretaceous old Lapurr series of massive arkosic sandstones, conglomerate layers and lacustrine shales, overlies an eroded surface of basement rocks (Arambourg, 1935), and in turn is overlain by Oligo-Miocene volcanics (Zanettin et al., 1983) (Fig. 4). An iron-oxide stained matrix of kaolinite, chlorite, muscovite and silica characterize this formation (Walsh & Dodson, 1969). Stratigraphic and petrographic similarities between the Lapurr, Anza and Sera Iltomia arkosic series may also suggest a similar age for these formations. The Lapurr and Anza sandstone series support the existence of a wide N140°-oriented axial fluvial system feeding from the North-West into the Anza Rift. In such a palaeoenvironmental context, the deposition of the Sera Iltomia sandstones would require a northerly oriented drainage pattern, possibly controlled by broadly N–S-trending faults similar to the ones present along the south-western margin of the Anza Rift (Morley et al., 1999c). Subsequent faulting in the Mount Porr area, that resulted in the intense deformation (normal faulting along the E–W and NNW–SSE trends, and also inversion tectonics) of the Sera Iltomia Formation, may have occurred during Palaeogene–middle Miocene (Morley, 1999c; Morley et al., 1999c).

The Sera Iltomia sandstones have porosities which range up to 33% and are a significantly better potential hydrocarbon reservoir than the Auwerwer/Lomerimong sandstones (max. 15% porosity). In both cases, significant burial diagenesis is absent so little porosity reduction can be ascribed to mechano-chemical diagenetic processes. Rather, the porosity of these sandstones is mainly controlled by their initial composition and structure and by early diagenetic chemical processes. Porosity variations can result from a variety of geological processes. Firstly, the clay matrix content is an important factor because a high clay matrix content limits the initial porosity and permeability and promotes mechanical compaction. Chemical processes induced from fluid flow can also play a role in porosity and permeability reduction. Quartz overgrowths and authigenic kaolin are only locally common in these sandstones, and, thus did not induce significant porosity reduction. In a few cases, early calcite cement completely occludes the initial porosity. However, in other cases, calcite cementation is only partial and instead has helped to preserve significant porosity by limiting mechanical compaction. Thus, the Sera Iltomia basement-derived sandstones, rather than the Auwerwer/Lomerimong sandstones, have the best potential to form good quality reservoirs. Nevertheless, the spatial relationships between such potential reservoirs and hydrocarbon-bearing rocks within the Turkana Depression have to be carefully explored.

5.3. Comparison with drilling results

The reservoir sandstones encountered in the different wells drilled in the Anza Rift (Figs. 2B and 4) have been briefly described by Winn et al. (1993) and Morley et al. (1999c). Below is a general description of these sandstones. The predominant type is arkose, with sub-ordinate sub-arkoses and litharenites, the composition of the rock fragments are predominantly granitic and metamorphic clasts. The sandstones are generally well to moderately sorted but subarkoses and litharenites tend to be more poorly sorted. Pore-filling constituents are detrital clay, calcite cement, quartz overgrowths, authigenic clay and dolomite. In certain wells the calcium zeolite laumontite is prevalent. The most commonly observed alteration is partial to complete replacement of feldspar grains and plutonic rock fragments by clay minerals and calcite, authigenic clay tends to predate quartz and calcite overgrowths. In exploration wells, sandstone porosity ranged from about 12 to 30% in the upper 1 km, 9–25% from 1 to 2 km, 5–18% from 2 to 3 km, and less than 10% below 3 km (Morley, 1999d). Generally, primary pore space below 3 km is uncommon. Secondary porosity (mostly from leached feldspar grains) is commonly developed below 2 km. The outcrop observations described above generally agree with the observations from the well data, and point to the importance of understanding the dynamics of fluid movements in rift basins.

Although the majority of sandstones follow a somewhat predictable pattern in the wells, two wells (Sirius-1 and Chalbi-1) (Figs. 2B and 4) are significantly different. The Sirius-1 well was drilled on top of a horst block, penetrating an older (Neocomian) section than surrounding wells. It encountered a 134 m thick sandstone, with a very low gamma ray response indicative of an atypically clean, quartz-rich sandstone with high porosity (15–20%). The dipmeter signature suggests internal dipping bedforms. The sandstone overlies a lacustrine carbonate sequence and probably represents an ancient aeolian dune field commonly associated with fluvial/lacustrine environments in rift systems (Breed et al., 1979; Morley et al., 1999c) (Fig. 12). This example illustrates that clean, porous quartz-rich sands, derived from basement sources occur within a rift environment.

The Chalbi-1 well is located 30 km from the Sirius-1 well (Fig. 2B) and is in a more basinal position, penetrating a thicker and younger section than the Sirius-1 well. The surprise with this well was the shallow reduction in porosity. Hence porosity was expected to be better at equivalent depths than in Sirius-1. However, below the depth of 1582 m in the Chalbi-1 well, porosity drops from 20–30% to 10%. This porosity reduction is caused by zeolites, particularly laumontite (Morley et al., 1999c). Chalbi-1 is near to the Huri Hills volcanic centre (Fig. 2B), known to have been active during late Miocene–Pliocene times (Key, 1987); hence it is likely that moderate to high temperature fluids related to this igneous centre interacted with the sandstones encountered in Chalbi-1 to produce the extensive laumontite cements (Morley et al., 1999c; Winn et al., 1993). This example illustrates the problems with trying to

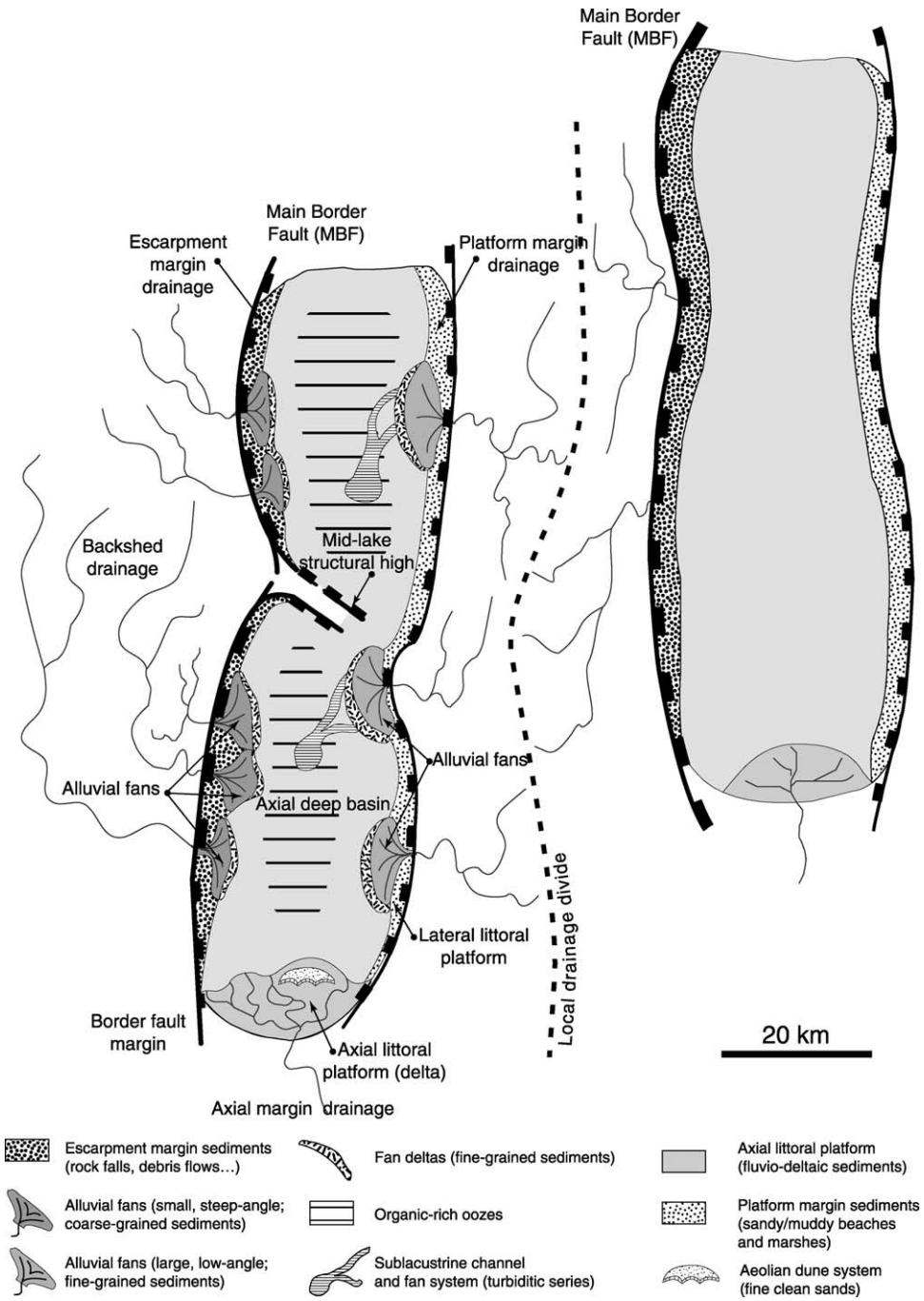

Fig. 12. Block-diagram illustrating a typical 'single half-graben' rift basin and its related faulted morphologies, drainages and distribution of main sedimentary bodies (modified from Cohen (1990) and Tiercelin et al. (1992, 1994)).

understand the effects of fluid movements in rift basins, and shows that the complex diagenetic history described from the outcrops also extends to the subsurface.

It has been noted that complex diagenetic events affect the syn-rift sandstones both as a result of their composition (alteration of feldspars and volcanic clasts) and by influx of migrating, commonly igneous-derived fluids. Our results suggest that hydrocarbon exploration needs to focus on reservoirs above 3000 m, and preferably above 2000 m depth. A few hydrocarbon fields exist in volcaniclastic rocks with much poorer reservoir potential (due to shallow diagenesis) than the rocks described here (e.g. Winut Field, Java; Kusumastuti, 1999). However, porosity was preserved due to the early migration of hydrocarbons into the reservoirs, which subsequently inhibited clay diagenesis. Given the high geothermal gradients typical in rifts, and the presence of thick, extensive syn-rift lacustrine shales (Morley et al., 1999b; see also companion paper) it is

by no means out of the question that early hydrocarbon migration could have preserved porosity against diagenetic events in some reservoirs in the rifts of Kenya.

6. Consequences of regional structure on reservoirs

The regional structural configuration played an important role in controlling the drainage from sediment source areas to the rift basin. Typically most rift sediment is derived either from axial or flexural margin sources, with a lesser contribution from the major boundary fault margin (Cohen, 1990; Tiercelin, Soreghan, Cohen, Lezzar, & Bouroullec, 1992, Tiercelin, Cohen, Soreghan, & Lezzar, 1994; Soreghan, Scholz, & Wells, 1999) (Fig. 12). For the Lokichar Basin, the axial sources would have been either from the south or the north. Input from the flexural margin to the east is likely to have been small since the North Kerio half-graben (Oligocene–Pliocene activity) lay to the east (Figs. 2B and 13A and B). The predominance of basement-derived quartz/feldspar-rich sand that comprises the Lokhone grits (Palaeogene–early Miocene) indicates that the sediment source was primarily from basement outcrops of granitic-composition to the south and south-east. This is confirmed by palaeocurrent data (Wescott et al., 1993) (Fig. 13A). Episodes of increased igneous contribution to the sandstone composition (Auwerwer Sandstone Formation) may reflect relatively minor volcanic events within the basin or onset of volcanism in previously basement-source areas outside the basin. In particular, the onset of volcanism around 23 Ma in the region of Samburu Basalts Formation south and southeast of the Lokichar Basin (Fig. 13B) appears to tie with the transition during the lower Miocene from the basement-derived Loperot Formation to the mixed basement and igneous-derived sources of the Auwerwer Sandstone Formation. To the north lay an extensive active volcanic province which stretched across the Lotikipi Basin (Figs. 2B and 13A) to the present-day east side of Lake Turkana (Fig. 13C). Also to the north, along-strike from the Lokichar Basin lies the east-thickening Lothidok Basin (Boschetto et al., 1992). During the late Oligocene–middle Miocene, lava flows, pyroclastics and volcaniclastic sediments issued from the igneous provinces situated to the north-north-west and north-east accumulated the Lothidok Basin (Figs. 2B, 13A and B). The conjugate convergent transfer zone between the two Lokichar and Lothidok basins served to separate two very different source areas for the basin fill, leaving the Lothidok Basin with very little reservoir potential and the Lokichar Basin with potential reservoir rocks sandstones.

The Lokichar Basin conforms with the typical stacking of continental rift facies where fluvio-deltaic sand-prone facies dominate deposition on the flexural margin and pass laterally into finer grained lacustrine facies towards the boundary fault margin (Cohen, 1990; Soreghan et al., 1999) (Fig. 12). Fine-grained overbank and ephemeral lake sequences interbedded with the sandstones are typically too thin and discontinuous to provide good seals for hydrocarbon traps. One of the key challenges for exploration in syn-rift basins is to find locations where thicker, more continuous basinal shales act as a seal for a potential reservoir. In the Lokichar Basin, the Lokhone and Loperot Shale Members represent fine-grained, organic-rich, extensive lacustrine high-stand intervals that have the potential to act as seals near the flexural margin, as it has been demonstrated in the Sharaf-Abu Gabra area (Muglad Rift; Fig. 2B) in Sudan (Mohamed, Pearson, Ashcroft, Iliffe, & Whiteman, 1999; Mohamed, Pearson, Ashcroft, &

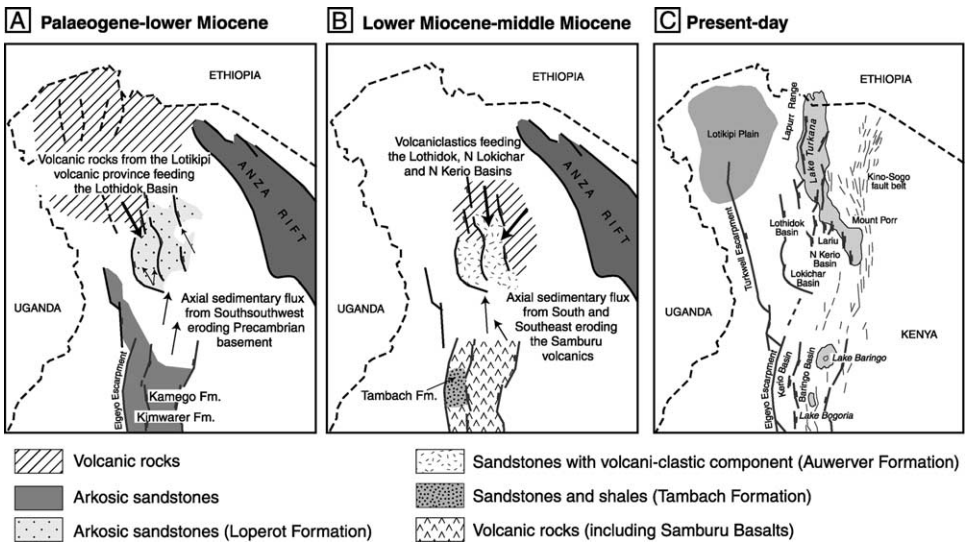

Fig. 13. Schematic drawings showing the tectono-sedimentary evolution and main sediment transport axes for the central-northern Kenya Rift: (A) From Palaeogene to lower Miocene. (B) From lower to middle Miocene. (C) Present-day structural setting of the central-northern Kenya Rift (modified after Morley et al. (1999b)).

Whiteman, 2002; Mohamed, 2002). These shales when buried deep enough are rich hydrocarbon source rocks (see companion paper).

As noted above, the Sera Iltomia Formation (as well as the nearby Lariu grits) may correspond with the Oligocene-early Miocene section imaged on the seismic lines in the Lokichar Basin. If so, the Sera Iltomia Formation may also be associated with potential source rocks which may be present in the nearby North Kerio Basin (Morley et al., 1999b) (Fig. 2B). Other potential source rocks have been encountered in the Lapurr Formation and in some of the wells drilled in the Anza Graben (Morley et al., 1999c; Winn et al., 1993). If associated with these various potential source rocks, the Sera Iltomia sandstones, with their good reservoir quality, can be considered as one of the best targets in the Turkana Depression, especially if they are sealed by lacustrine shales or mudstones linked to the development of lake basins during early-middle Cenozoic.

7. Conclusion

Outcrop studies of the reservoir characteristics in syn-rift sandstones of the Auwerwer/Lomerimong and Seria Iltomia Formations have highlighted significant potential lateral and vertical variations in reservoir quality. Sandstones of a completely different composition may accumulate in adjacent basins because of differences in sediment source areas. Significant vertical variations in the composition of the reservoirs is common as sediment source areas change with time. Likely variations in source area are due to: (1) covering of an existing basement source area with extrusive volcanism; (2) erosion through igneous cover rocks into basement; and 3) structural or tectonic uplift, or reorganisation of fault patterns, that result in changes to drainage patterns and thus source areas. Much of the sediment transport in rifts is short, resulting in poorly sorted litharenites, arkoses and subarkoses. However there is occasionally the potential for finding clean sandstones (e.g. Sirius-1 well), possibly related to other types of transport processes (aeolian) associated with wide fluvial/lacustrine systems in a rift setting. The mixed sediment source means a variety of diagenetic effects can occur that reduce primary porosity and permeability non-uniformly, and sometimes promote secondary porosity. Diagenetic effects in sandstones are greatest where there is a considerable volcanic component. Outcrop examples show that even at shallow depths of burial early diagenetic events probably related to migrating fluids (related to volcanism and possibly seismic pumping along faults) can significantly reduce porosity. In addition, zeolite (laumontite) cements derived from alteration of feldspars and volcanic clasts by hydrothermal fluids are common in the subsurface. It is probable that early migration of hydrocarbons into reservoir units could inhibit laumontite cements, but calcite-analcite cementation may occur too shallow and early for hydrocarbon traps to be in place (less than 1 km).

Acknowledgements

This study represents part of a cooperative program conducted with the National Oil Corporation of Kenya (NOCK), and funded by the 3D-3G Project supported by Elf Petroleum Norge AS (grant No 2231-01 ELF to J.-J. Tiercelin), as well as by grants from SUCRI-2E and UMR CNRS 6538 'Domaines Océaniques', European Institute of Marine Studies, University of Western Brittany, Brest, France. Research authorization was provided by the Office of the President of the Republic of Kenya. Special thanks are due to NOCK Managing Director for permission to publish this work, and to Dr F.M. Mbatau, NOCK Exploration and Production Manager, for scientific, administrative and logistic support. The authors are grateful to W. Bosworth and an anonymous referee for constructive revisions of the manuscript, M. Soreghan for text improvement, and B. Coléno for constant assistance with illustrations. This is publication No 149 of the International Decade of East African Lakes (IDEAL) programme.

References

Arambourg, C. (1933). Mammifères Miocènes du Turkana (Afrique Orientale). *Annales Paléontologie*, *22*, 123–146.

Arambourg, C. (1935). *Esquisse géologique de la bordure occidentale du Lac Rodolphe. Mission Scientifique de l'Omo 1932-3* (*Vol. I(1)*). *Muséum National d'Histoire Naturelle, Paris*, 59 pp.

Arambourg, C. (1943). *Contribution à l'étude géologique et paléontologique du Bassin du Lac Rodolphe et de la Basse Vallée de l'Omo. Mission Scientifique de l'Omo.* (*Vol. I(2)*). *Muséum National d'Histoire Naturelle, Paris*, pp. 157–230.

Arambourg, C., & Wolff, R. G. (1969). Nouvelles données paléontologiques sur l'âge des grès du Lubur (Turkana grits) à l'Ouest du lac Rodolphe. *Comptes Rendus Société géologique de France*, *6*, 190–202.

Baker, B. H., & Wohlenberg, J. (1971). Structure and evolution of the Kenya Rift Valley. *Nature*, *229*, 538–542.

Baker, B. H., Mohr, P. A., & Williams, L. A. J. (1972). *Geology of the Eastern Rift System of Africa. Geological Society of America Special Paper, 136*, pp. 67.

Bellieni, G., Justin Visentin, E., Zanettin, B., Piccirillo, E. M., Radicati di Brozolo, F., & Rita, F. (1981). Oligocene transitional-tholeiitic magmatism in northern Turkana (Kenya). Comparison with the coeval Ethiopian volcanism. *Bulletin of Volcanology*, *44*, 411–427.

Boschetto, H. B (1988). *Geology of the Lothidok Range, Northern Kenya*. MS Thesis. Department of Geology and Geophysics, University of Utah.

Boschetto, H. B., Brown, F. H., & McDougall, I. M. (1992). Stratigraphy of the Lothidok Range, northern Kenya, and K/Ar ages of its Miocene primates. *Journal of Human Evolution*, *22*, 47–71.

Bosworth, W. (1992). Mesozoic and Early Tertiary rift tectonics in East Africa. *Tectonophysics*, *209*, 115–137.

Bosworth, W., & Maurin, A. (1993). Structure, geochronology and tectonic significance of the northern Suguta Valley (Gregory Rift), Kenya. *Journal of the Geological Society, London*, *150*, 751–762.

Bosworth, W., & Morley, C. K. (1994). Structural and stratigraphic evolution of the Anza rift, Kenya. In C. Prodehl, G. R. Keller, & M. A. Khan (Eds.), *Crustal and Upper Mantle Structure of the Kenya Rift* (*Vol. 236*) (pp. 93–115). *Tectonophysics*.

Breed, C. S., Fryberger, S. C., Andrews, S., McCauley, C., Lennartz, F., Gebel, D., & Horstman, K. (1979). Regional studies of sand seas using Landsat (ERTS) imagery. In E. D. McKee (Ed.), *Global sand seas* (*Vol. 1052*) (pp. 305–397). *Prof. Paper US Geological Survey*.

Buatier, M. D., Potdevin, J.-L., Lopez, M., & Petit, S. (1996). Occurrences of nacrite in the Lodève Permian basin (France). *European Journal of Mineralogy*, *8*, 847–852.

Chapman, G. R., & Brook, M. (1978). Chronostratigraphy of the Baringo basin, Kenya Rift Valley. In W. W. Bishop (Ed.), *Geological background to fossil man* (pp. 207–223). Edinburgh: Scottish Academic.

Chapman, G. R., Lippard, S. J., & Martyn, J. E. (1978). The stratigraphy and structure of the Kamasia Range, Kenya Rift Valley. *Journal of the Geological Society, London*, *135*, 265–281.

Cohen, A. S. (1990). Tectono-stratigraphic model for sedimentation in Lake Tanganyika, Africa. In B. J. Katz (Ed.), *Lacustrine basin exploration: case studies and modern analogs* (pp. 137–150). *AAPG Memoir, 50*.

Dodson, R. G. (1971). *Geology of the area south of Lodwar. Report Geological Survey of Kenya, 87*, 36 pp.

Dunkelman, T. J., Karson, J. A., & Rosendahl, B. R. (1988). Structural style of the Turkana Rift, Kenya. *Geology*, *16*, 258–261.

Dunkelman, T. J., Rosendahl, B. R., & Karson, J. A. (1989). Structure and stratigraphy of the Turkana rift from seismic reflection data. *Journal of African Earth Sciences*, *8*, 489–510.

Dunkley, P. N., Smith, M., Allen, D. J., & Darling, W. G. (1993). *The geothermal activity and geology of the northern sector of the Kenya Rift Valley. British Geological Survey Research Report SC/93/1*, 185 pp.

Ebinger, C. J., & Ibrahim, A. (1994). Mutiple episodes of rifting in Central and East Africa: A re-evaluation of gravity data. *Geological Rundschau*, *83*, 689–702.

Ebinger, C. J., Yemane, T., Harding, D. J., Tesfaye, S., Kelley, S., & Rex, D. C. (2000). Rift deflection, migration, and propagation: Linkage of the Ethiopian and eastern rifts, Africa. *Bulletin of the Geological Society of America*, *112*, 163–176.

Feibel, C. S (1988). *Paleoenvironments of the Koobi Fora Formation, Turkana Basin, Northern Kenya*. PhD Thesis. Utah University.

Feibel, C. S., Harris, J. M., & Brown, F. H. (1991). Neogene paleoenvironments of the Turkana Basin. In J. M. Harris (Ed.), *Koobi Fora Research Project, Vol. 3, Stratigraphy, artiodactyls and paleoenvironments* (pp. 321–346). Oxford: Clarendon Press.

Fleet, A. J., Kelts, K., & Talbot, M. R. (1988) (*Vol. 40*). *Lacustrine petroleum source rocks*, London: Geological Society Special Publication, 391 pp.

Fuchs, V. E. (1939). The geological history of the Lake Rudolf Basin, Kenya Colony. *Philosophical Transaction of the Royal Society of London*, *229*, 219–274.

Geological Map of Kenya (1987). 1:1,000,000. Published by the Ministry of Energy and Regional Development of Kenya.

Gibling, M. R. (1988). Cenozoic lacustrine basins of South-East Asia, their tectonic setting, depositional environment and hydrocarbon potential. In A. J. Fleet, K. Kelts, & M. R. Talbot (Eds.), (*Vol. 40*) (pp. 341–351). *Lacustrine petroleum source rocks*, London: Geological Society Special Publication.

Golden, M (1978). *The geology of the area east of Silale, Rift Valley Province, Kenya*. PhD Thesis. University of London (Unpublished) (pp. 254).

Grall, M (2000). Le lac Bogoria, Rift Central du Kenya: Reconstitution paléogéographique et intérêt pétrolier d'un bassin de rift à partir d'une série sédimentaire Pléistocène supérieur-Holocène. DEA Université de Bretagne Occidentale. 49 pp.

Guiraud, R., & Bosworth, W. (1997). Senonian basin inversion and rejuvenation of rifting in Africa and Arabia: synthesis and implications to plate-scale tectonics. *Tectonophysics*, *282*, 39–82.

Greene, L. C., Richards, D. R., & Johnson, R. A. (1991). Crustal structure and tectonic evolution of the Anza rift, northern Kenya. *Tectonophysics*, *197*, 203–211.

Hackman B.D (1988). *Geology of the Baringo-Laikipia area*. Report 104. Republic of Kenya, Ministry of Environment and Natural Resources, Mines and Geological Department (pp. 79).

Harris, N., Pallister, J. W., & Brown, J. M. (1956). Oil in Uganda. *Geological Survey of Uganda*, *9*, 33.

Hassouta, L., Buatier, M., Potdevin, J.-L., & Liewig, N. (1999). Clay diagenesis in the sandstone reservoir of the Ellon Field (Alwyn, North Sea). *Clays Clay Mineralogy*, *47*, 269–285.

Hautot, S., Tarits, P., Whaler, K., Le Gall, B., Tiercelin, J.-J., & Le Turdu, C. (2000). Deep structure of the Baringo Rift Basin (central Kenya) from three-dimensional magnetotelluric imaging: implications for rift evolution. *Journal of Geophysical Research*, *105*(B10), 23493–23518.

Herbin, J. P. (1979). Sédimentation de rift: Géochimie organique des sédiments récents du lac Bogoria. *Rapport Institut Français du Pétrole 26881*, 20.

Höhnel, L. R. von, Rosiwal, A., Toula, F., & Suess, E. (1891). Beiträge zur geologischen Kenntniss des Östlichen Afrika. *Denkschriften der Kaiserlichen Akademie der Wissenschaften, Mathematish-Naturwissens Chafliche Klasse*, *58*, 447–584.

Huc, A. Y., Le Fournier, J., Vandenbroucke, M., & Bessereau, G. (1990). Northern Lake Tanganyika—An example of organic sedimentation in an anoxic rift lake. In B. J. Katz (Ed.), *Lacustrine basin exploration—case studies and modern analogs* (pp. 169–185). *AAPG Memoir, 50*.

Joubert, P. (1966). *Geology of the Loperot area. Report Geological Survey of Kenya, 74*, 52 pp.

Katz, B. J. (1988). Clastic and carbonate lacustrine systems: An organic geochemical comparison (Green River Formation and East African lake sediments). In A. J. Fleet, K. Kelts, & M. R. Talbot (Eds.), (*Vol. 40*) (pp. 81–90). *Lacustrine petroleum source rocks*, London: Geological Society Special Publication.

Katz, B. J. (1990). Controls on distribution of lacustrine source rocks through time and space. In B. J. Katz (Ed.), *Lacustrine basin exploration—case studies and modern analogs* (pp. 61–76). *AAPG Memoir 50*.

Katz, B. J. (1995). A survey of rift basin source rocks. In J. J. Lambiase (Ed.), (*Vol. 80*) (pp. 213–242). *Hydrocarbon habitat in rift basins*, London: Geological Society Special Publication.

Key, R. M (1987). *Geology of the Marsabit area*. Report 108 (Reconnaissance). Republic of Kenya, Ministry of Environment and Natural Resources, Mines and Geological Department (pp. 42).

Kusumastuti, A. (1999). The Wunut Field: Pleistocene volcaniclastic gas sands in East Java. *Proceedings of the Indonesian Petroleum Association, Jakarta*, 195–205.

Lambiase, J. J. (1989). The framework of African rifting during the Phanerozoic. *Journal of African Earth Sciences*, *8*, 183–190.

Lambiase, J. J. (1995) (*Vol. 80*). *Hydrocarbon Habitat in Rift Basins*, London: Geological Society Special Publication, pp. 381.

Maglio, V. J. (1969). A shovel-tusked Gomphotere from the Miocene of Kenya. *Museum Comparative Zoollogy Breviora*, *310*, 1–10.

Mahood, G. A., & Drake, R. E. K-A. r. (1982). dating young rhyolitic rocks: a case study of the Sierra la Primavera, Mexico. *Geological Society of America Bulletin*, *93*, 1232–1241.

Marshall, D. J. (1988). Cathodoluminescence of geological materials. London: Unwin Hyman, 66 pp.

McHargue, T. R., Heidrick, T. L., & Livingston, J. E. (1992). Tectonostratigraphic development of the Interior Sudan rifts, Central Africa. *Tectonophysics*, *213*, 187–202.

Mead, J. G. (1975). A fossil beaked whale (Cetacea: Ziphiidae) from the Miocene of Kenya. *Journal of Palaeontology*, *49*, 745–751.

Mohamed, A. Y. (2002). Petroleum maturation modelling, Abu Gabra-Sharaf area, Muglad Basin, Sudan. *Journal of African Earth Sciences*, *35*, 331–344.

Mohamed, A. Y., Pearson, M. J., Ashcroft, W. A., Iliffe, J. E., & Whiteman, A. J. (1999). Modeling petroleum generation in the southern Muglad rift basin, Sudan. *AAPG Bulletin*, *83*, 1943–1964.

Mohamed, A. Y., Pearson, M. J., Ashcroft, W. A., & Whiteman, A. J. (2002). Petroleum maturation modelling, Abu Gabra-Sharaf area, Muglad Basin, Sudan. *Journal of African Earth Sciences*, *35*, 331–344.

Morimoto, I. M. (1988). Nomenclature of pyroxenes. *Mineralogical Magazine*, *52*, 535–550.

Morley, C. K. (1995). Developments in the structural geology of rifts over the last decade and their impact on hydrocarbon exploration. In J. J. Lambiase (Ed.), (*Vol. 80*) (pp. 1–32). *Hydrocarbon habitat in rift basins*, London: Geological Society Special Publication.

Morley, C. K. (1999b). Basin evolution trends in East African rifts. In C. K. Morley (Ed.), *Geoscience of rift systems—evolution of East Africa* (*Vol. 44*) (pp. 131–150). *AAPG Studies in Geology*.

Morley, C. K. (1999c). Tectonic inversion in East African rifts. In C. K. Morley (Ed.), *Geoscience of rift systems—evolution of East Africa* (*Vol. 44*) (pp. 193–210). *AAPG Studies in Geology*.

Morley, C. K. (1999d). Comparison of hydrocarbon prospectivity in rift systems. In C. K. Morley (Ed.), *Geoscience of rift systems—evolution of East Africa* (*Vol. 44*) (pp. 233–242). *AAPG Studies in Geology*.

Morley, C. K., Wescott, W. A., Stone, D. M., Harper, R. M., Wigger, S. T., & Karanja, F. M. (1992). Tectonic evolution of the northern Kenyan Rift. *Journal of the Geological Society, London*, *149*, 333–348.

Morley, C. K., Wescott, W. A., Stone, D. M., Harper, R. M., Wigger, S. T., Karanja, F. M., & Day, R. A. (1999b). Geology and geophysics of the western Turkana basins. In C. K. Morley (Ed.), *Geoscience of rift systems—evolution of East Africa* (*Vol. 44*) (pp. 19–54). *AAPG Studies in Geology*.

Morley, C. K., Day, R. A., Lauck, R., Bosher, R., Stone, D. M., Wigger, S. T., Wescott, W. A., Haun, D., Bassett, N., & Bosworth, W. (1999c). Geology and geophysics of the Anza Graben. In C. K. Morley (Ed.), *Geoscience of rift systems—evolution of East Africa* (*Vol. 44*) (pp. 67–90). *AAPG Studies in Geology*.

Mugisha, F., Ebinger, C. J., Strecker, M., & Pope, D. (1997). Two-stage rifting in the Kenya Rift: implications for half-graben models. *Tectonophysics*, *278*, 61–81.

Murray-Hughes, R. (1933). *Notes on the geological succession, tectonics and economic geology of the western half of Kenya Colony* (*Vol. 3*). *Report Geological Survey of Kenya*, 8 pp.

Peterson, J. A. (1986). Geology and petroleum resources of central and east-central Africa. *Modern Geology*, *10*, 329–364.

Qiu, Y., Xue, P., & Xiao, J. (1987). Fluvial sandstone bodies as hydrocarbon reservoirs in lake basins. *The Society of Economic Paleontologists and Mineralogists*, *39*, 329–342.

Reid, R. P., Macintyre, I. G., & Post, P. E. (1992). Micritized skeletal grains in northern Belize lagoon: a major source of Mg-calcite mud. *Journal of Sedimentary Petrology*, *62*, 145–156.

Renaut, R. W., Ego, J., Tiercelin, J.-J., Le Turdu, C., & Owen, B. (1999). Saline, alkaline palaeolakes of the Tugen Hills-Kerio Valley region, Kenya Rift Valley. In P. Andrews, & P. Banham (Eds.), *Late Cenozoic environments and hominid evolution: a tribute to Bill Bishop* (pp. 41–58). London: Geological Society.

Roche, H., Delagnes, A., Brugal, J.-P., Feibel, C., Kibunjia, M., Mourre, V., & Texier, P.-J. (1999). Early hominid stone tool production and technical skill 2.34 Myr ago in Wets Turkana, Kenya. *Nature*, *399*, 57–60.

Savage, R. J. G., & Williamson, P. G. (1978). The early history of the Turkana depression. In W. W. Bishop (Ed.), *Geological background to fossil man* (pp. 375–394). Edinburgh: Scottish Academic.

Schull, T. J. (1988). Rift basins of interior Sudan: Petroleum exploration and discovery. *AAPG Bulletin*, *72*, 1128–1162.

Shackleton, R. M. (1946). Geology of the country between Nanyuki and Maralal. *Report Geological Survey of Kenya*, 11.

Simoneit, B. R. T., Aboul-Kassim, T. A. T., & Tiercelin, J.-J. (2000). Hydrothermal petroleum from lacustrine sedimentary organic matter in the East African Rift. *Applied Geochemistry*, *15*, 355–368.

Smith, M., & Mosley, P. (1993). Crustal heterogeneity and basement influence on the development of the Kenya Rift, East Africa. *Tectonics*, *12*, 591–606.

Soreghan, M. J., Scholz, C. A., & Wells, J. T. (1999). Coarse-grained, deep-water sedimentation along a border fault margin of Lake Malawi, Africa: seismic stratigraphic analysis. *Journal of Sedimentary Research*, *69*, 832–846.

Steiger, R. H., & Jäger, E. (1978). Subcommission on geochronology: convention on the use of decay constants in geo- and cosmochronology. *Earth and Planetary Science Letters*, *36*, 359–362.

Talbot, M. R. (1988). The origins of lacustrine oil source rocks: evidence from the lakes of tropical Africa. In A. J. Fleet, K. Kelts, & M. R. Talbot (Eds.), (*Vol. 40*) (pp. 29–43). *Lacustrine petroleum source rocks*, London: Geological Society Special Publication.

Tiercelin, J.-J. (1991). Natural resources in the lacustrine facies of the Cenozoic rift basins of East Africa. *Special Publication International Association of Sedimentologists*, *13*, 3–37.

Tiercelin, J.-J., & Vincens, A. (1987). Le demi-graben de Baringo-Bogoria, Rift Gregory, Kenya. 30,000 ans d'histoire hydrologique et sédimentaire. *Bulletin des Centres de Recherches Exploration—Production Elf Aquitaine*, *11*, 249–540.

Tiercelin, J.-J., Soreghan, M. J., Cohen, A. S., Lezzar, K. E., & Bouroullec, J.-L. (1992). Sedimentation in large rift lakes: example from the Middle Pleistocene-Modern deposits of the Tanganyika trough, East African Rift System. *Bulletin des Centres de Recherches Exploration-Production Elf Aquitaine*, *16*, 83–111.

Tiercelin, J.-J., Pflumio, C., Castrec, M., Boulègue, J., Gente, P., Rolet, J., Coussement, C., Stetter, K. O., Huber, R., Buku, S., & Mifundu, W. (1993). Hydrothermal vents in Lake Tanganyika, East African Rift system. *Geology*, *21*, 499–502.

Tiercelin, J.-J., Cohen, A. S., Soreghan, M. J., & Lezzar, K. E. (1994). Pleistocene-modern deposits of the Lake Tanganyika Rift Basin, East Africa: A modern analog for lacustrine source rocks and reservoirs. In A. J. Lomando, B. C. Schreiber, & P. M. Harris (Eds.), *Lacustrine reservoirs and depositional systems* (pp. 37–59). *SEPM Core Workshop No. 19*.

Vétel, W., Le Gall, B., Tiercelin, J.-J., Johnson, T. C., Collet, B (submitted for publication). Active tectonics in the Turkana Rift (North Kenya): an integrated approach from drainage network, satellite imagery and reflection seismic analyses.

Vicat, J.-P., & Pouclet, A. (1995). Nature du magmatisme lié à une extension pré-panafricaine: les dolérites des bassins de Comba et Sembe-Ouesso (Congo). *Bulletin de la Société géologique de France*, *166*, 355.

Walsh, J. (1969). Geology of the Eldama Ravine-Kabarnet area. *Report Geological Survey of Kenya*, 83.

Walsh, J., & Dodson, R. G. (1969). Geology of Northern Turkana. *Report Geological Survey of Kenya*, 82.

Wescott, W. A., Morley, C. K., & Karanja, F. M. (1993). Geology of the 'Turkana Grits' in the Lariu Range and Mt Porr areas, southern Lake Turkana, Northwestern Kenya. *Journal of African Earth Sciences*, *16*, 425–435.

Williamson, P. G., & Savage, R. J. G. (1986). Early rift sedimentation in the Turkana basin, northern Kenya. In L. E. Frostick, R. W. Renaut, I. Reid, & J.-J. Tiercelin (Eds.), (*Vol. 25*) (pp. 267–283). *Sedimentation in the African Rifts*, London: Geological Society Special Publication.

Winn, R. D., Steinmetz, J. C., & Kerekgyarto, W. L. (1993). Stratigraphy and rifting history of the Anza Rift. *AAPG Bulletin*, *77*, 1989–2005.

Zanettin, B., Justin Visentin, E., Bellieni, G., Piccirillo, E. M., & Zanettin, B. (1983). Le volcanisme du Bassin du Nord-Turkana (Kenya): Age, succession et évolution structurale. *Rifts et Fossés anciens* (*7*) (pp. 249–255). *Bulletin des Centres de Recherches Exploration-Production Elf-Aquitaine*.